DOE/MC/10637-3664
(DE94004080)
4064

Low-Rank Coal Research

Quarterly Report
January - March 1990

August 1990

Work Performed Under Contract No.: DE-FC21-86MC10637

For
U.S. Department of Energy
Office of Fossil Energy
Morgantown Energy Technology Center
Morgantown, West Virginia

By
University of North Dakota
Energy and Environmental Research Center
Grand Forks, North Dakota

DOE/MC/10637-3664
(DE94004080) 4064
Distribution Category UC-105

Low-Rank Coal Research

Quarterly Report
January - March 1990

Work Performed Under Contract No.: DE-FC21-86MC10637

For
U.S. Department of Energy
Office of Fossil Energy
Morgantown Energy Technology Center
P.O. Box 880
Morgantown, West Virginia 26507-0880

By
University of North Dakota
Energy and Environmental Research Center
P.O. Box 9018
Grand Forks, North Dakota 58202

August 1990

TABLE OF CONTENTS

2.0 CONTROL TECHNOLOGY AND COAL PREPARATION RESEARCH

2.1 Flue Gas Cleanup

FLUE GAS CLEANUP

Quarterly Technical Progress Report
for the Period January - March 1990

by

Greg F. Weber, Project Manager
Stanley J. Miller, Senior Research Engineer
Dennis L. Laudal, Research Engineer
Energy and Environmental Research Center
Box 8213, University Station
Grand Forks, ND 58202

Contracting Officer's Technical Representative: Perry Bergman

for

U.S. Department of Energy
Pittsburgh Energy Technology Center
P.O. Box 10940
Pittsburgh, PA 15236-0940

May 1990

Work Performed Under Cooperative Agreement No. DE-FC21-86MC10637

TABLE OF CONTENTS

LIST OF FIGURES

List of Figures (continued)

LIST OF TABLES

FLUE GAS CLEANUP

1.0 INTRODUCTION

The objective of the Department of Energy (DOE) Flue Gas Cleanup Program, under the direction of the Pittsburgh Energy Technology Center (PETC), is to promote the widespread use of coal. This is to be accomplished by providing the technology necessary for utilization of coal in an environmentally and economically acceptable manner. The program addresses the reduction of acid rain precursor emissions as well as developing technologies with the potential to meet more stringent emissions control requirements for SO_2, NO_x, and particulate matter.

Activities within the Energy & Environmental Research Center's (EERC's) Cooperative Agreement Flue Gas Cleanup Project address the advanced NO_x control and fine particulate control areas of the DOE Flue Gas Cleanup Program. Specific activities involve the development of a catalytic fabric filter for NO_x and particulate control and methods to measure the cohesive strength and reentrainment potential of fly ashes relative to fine particle emissions from fabric filters.

2.0 GOALS AND OBJECTIVES

The overall objective of the catalytic fabric filter effort is the development of a catalytic fabric filter for NO_x and particulate control that will provide high removal efficiency of NO_x and particulate matter, acceptably long bag and catalyst life, and an economic savings over a conventional SCR system and baghouse. The specific goals of the program are to develop a catalytic fabric that will provide:

- 90% NO_x removal with <25 ppm ammonia slip.
- A particulate removal efficiency of >99.5%.
- A bag/catalyst life of >1 year.
- A 20% cost savings over conventional baghouse and SCR control technology.
- Compatibility with SO_2 removal systems.
- A nonhazardous waste material.

The general objective of the fine particulate control effort is to develop methods to help characterize, control, and model fine particulate emissions from a fabric filter. Characterization efforts include the development of methods to measure the cohesive strength and reentrainment potential of fly ashes. Control and modeling efforts involve relating these parameters to the level of fine particle emissions from fabric filters. Specific goals for the next year include the following:

- Evaluate existing methods and select or develop reliable methods to measure the cohesive strength of fly ash.

- Correlate measured cohesive strength with other ash properties such as particle size, particle shape, surface area, porosity, and ash chemistry.

- Measure reentrainment potential of ash from the surface of a fly ash filter cake or bulk fly ash and relate it to the measured cohesive strength.

Specific project activities to be completed during the fourth year of the Cooperative Agreement include the following:

- Perform project planning activities and develop a detailed statement of work for the fourth year of the Cooperative Agreement (July 1, 1989, through June 30, 1990).

- Perform bench-scale catalytic fabric screening tests using actual flue gas from pulverized coal combustion.

- Initiate planning for catalytic filter bag evaluation and parametric tests.

- Review methods to measure the cohesive strength of bulk fly ash and evaluate selected methods by generating cohesive strength data for both conditioned and nonconditioned fly ash, comparing the data with other measurable fly ash properties.

- Construct a bench-scale fly ash reentrainment device to perform bench-scale tests quantifying reentrainment behavior for both conditioned and nonconditioned fly ash.

Specific project activities during the third quarter of the fourth year of the Cooperative Agreement included the following:

- Complete Task B, including the evaluation of the effects of coal type on catalyst-coated fabrics.

- Complete analysis of catalyst-coated fabric samples used for Task B testing. Specifically, determine the vanadium concentration and monosorb BET surface area for each fabric sample.

- Initiate tests using the fly ash reentrainment system.

3.0 ACCOMPLISHMENTS

3.1 Task B -- Fabric Screening Tests

3.1.1 Facilities and Procedures

To minimize the amount of construction necessary prior to testing, the 0.8-ft^2 fabric filter holder and oven used in Task A were used as part of the slipstream system in Task B. The slipstream sample system was designed and constructed such that a portion of the flue gas produced from a 550,000-Btu/hr pc-fired combustor (PTC) was drawn through a filter sample at the required

air-to-cloth ratio and measured using a calibrated orifice. After the filter, the flow was split three ways. One stream was sent to a sample conditioner and flue gas analyzers, a second stream was used to measure ammonia/SO_3, and the balance of the flue gas was sent to a gas pump and dry gas meter to control the total system flow. A schematic of the slipstream sample system is shown in Figure 1.

Pressure drop across the filter was measured continuously. Periodically, it was necessary to clean the filter during some of the tests. To do this, the gas flow was reversed through the filter sample, causing the dust cake to be disturbed. Although the dust was not actually removed from the filter, this approach was sufficient to keep the pressure drop at a manageable level.

The ammonia flow rate to the combustion system was determined by first measuring the total flue gas flow rate with a calibrated orifice and/or Annubar flow measuring device. Then the amount of ammonia needed was calculated, based on the initial NO_x baseline value. The inlet ammonia flow rate was controlled using a mass flow meter with an automatic controller.

Ammonia was injected into the center of the 3.625-inch diameter flue gas duct through a nozzle that consisted of a 1/4-inch stainless steel closed end tube with six 0.028-inch diameter holes around the circumference of its tip. This injection configuration along with a flue gas Reynolds number of about 29,000 provided adequate mixing of the ammonia and the flue gas prior to drawing a flue gas sample through the slipstream sample system.

To provide on-line NO_x analyses, instrumentation included two Thermo Electron Model 10 Chemiluminescent NO_x Analyzers with molybdenum converters. The approach used to determine the amount of NO_x was to monitor the NO_x after the slipstream sample system (prior to starting the ammonia injection) to establish a baseline reading. At the end of the test, the ammonia was shut off to again establish the baseline readings. An NO_x analyzer at the combustor exit was used to record fluctuations in the total NO_x concentration entering the slipstream sample system.

Other on-line gas analysis instrumentation included two Beckman Model 755 O_2 analyzers, two Dupont Model 400 SO_2 analyzers, a Beckman Model 865 CO_2 analyzer, and a Beckman Industrial Model 880 CO analyzer. The flue gas was continually sampled both prior to and following the slipstream sample system. Heat-traced line was used prior to the sample conditioners to prevent water condensation in the sample lines. All gas monitoring instrumentation were routinely calibrated with certified span gases.

Data, including gas concentrations, system temperatures, and pressures, were automatically logged by use of a Kaye data logger and circle charts. Also, backup data were routinely recorded in a log book by the operators.

Ammonia and SO_3 were measured using wet chemistry methods. Ammonia was extracted from the flue gas stream using a pump and then bubbled through dilute sulfuric acid where the ammonia was absorbed. The dissolved ammonia content was then measured using a specific ion electrode, after bringing the pH of the solution to 11 with sodium hydroxide. The total volume of flue gas sampled was measured using a dry gas meter.

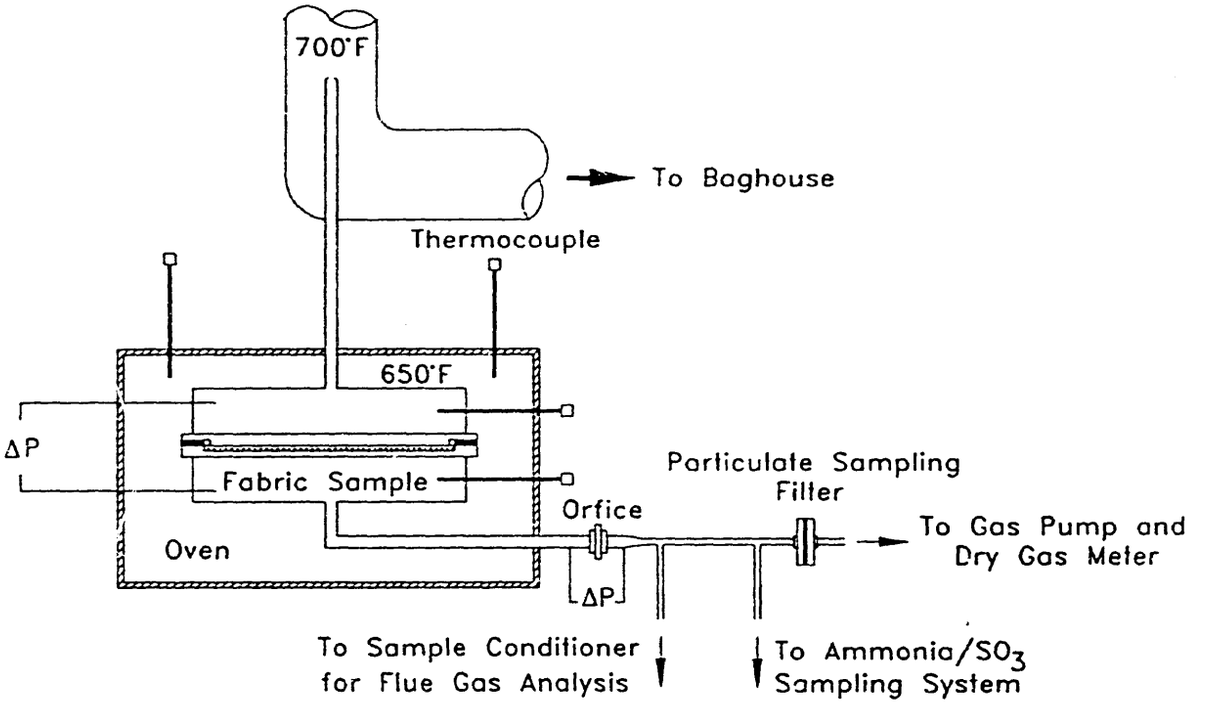

Figure 1. Schematic of slipstream sample system.

SO_3 was measured using the selective condensation procedure where the flue gas is passed through a condenser at a temperature maintained between 140° and 190°F. In this range the SO_3 (sulfuric acid) is condensed while all other flue gas constituents remain in the gas phase. The condensate is then rinsed from the condenser and the SO_3 concentration determined by titration.

3.1.2 Results and Discussion

Four coals were selected for use during Task B experiments to determine the effects of coal type on the catalyst-coated fabric performance (NO_x removal efficiency and ammonia slip). These included a medium sulfur washed Illinois #6 bituminous, a high sulfur Pyro Kentucky bituminous, a Jacobs Ranch subbituminous, and a South Hallsville, Texas. lignite. The ultimate and proximate analyses for each of the coals are presented in Table 1. The washed Illinois #6 bituminous coal was the baseline coal used for the fabric screening tests reported in the October through December 1989 Quarterly Technical Progress Report.

Following the fabric screening tests, two fabrics, fabrics #2 and #13, were selected to be tested using the remaining three coals. For the first 6 hours of each test the air-to-cloth ratio was held constant at 3 ft/min. However, near the end of each test, the air-to-cloth ratio was adjusted to 2 ft/min and to 4 ft/min, respectively, for 1 hour. The ammonia/NO_x molar ratio was 0.9 for all the tests. Table 2 summarizes the test results while firing each of the four coals for fabrics #2 and #13. The data is also represented graphically in Figures 2 through 7.

TABLE 1

ANALYSES OF COALS USED IN TASK B
(On an As-Received Basis)

	Washed Illinois #6	Kentucky Pyro	Wyodak Jacobs Ranch	South Hallsville
Coal Type	Bituminous	Bituminous	Subbituminous	TX Lignite
Proximate Analysis, wt%				
Moisture	13.7	5.9	23.1	36.8
Volatile Matter	32.8	31.7	33.0	23.6
Fixed Carbon	43.2	48.1	38.5	29.8
Ash	10.3	13.3	5.5	9.6
Ultimate Analysis, wt%				
Hydrogen	5.8	5.5	6.8	6.6
Carbon	61.0	65.6	52.5	39.8
Nitrogen	1.0	1.3	0.7	0.5
Sulfur	2.7	4.6	0.3	1.3
Oxygen (Diff.)	19.2	9.7	34.2	42.2
Ash	10.3	13.3	5.5	9.6
Heating Value (Btu/lb)	10,819	11,857	9,129	6,719

Ammonia slip measurements and SO_3 concentrations were made for each test. In addition, for the Pyro Kentucky bituminous coal, the concentration of HCl was measured due to high levels of chlorine in the coal (0.2%). As a baseline, an HCl measurement was also made using South Hallsville, which has very low chlorine content. The ammonia slip was higher than would be expected for several of the tests. Therefore, it is likely the ammonia/NO_x molar ratio was not as constant as would have been desired. There was some instability in the combustion process which resulted in NO_x readings that were ± 50 ppm, and it was not always possible to adjust the ammonia flow rate to correct for this change.

To get a more accurate indication of the SO_3 concentration in the flue gas, the ammonia was turned off during the time when the SO_3 measurements were made. During this time, the NO_x removal efficiency went to zero, as is shown in Figures 2 through 5. Although the ammonia was not on, the SO_3 concentrations were still extremely low (<2 ppm) for all the tests. This result was somewhat unexpected, especially for the high sulfur coal (3800 ppm SO_2 in the flue gas) Pyro Kentucky Bituminous. A more detailed evaluation of SO_3 measurement techniques is needed.

TABLE 2

RESULTS FROM TASK B -- EFFECTS OF COAL TYPE

Fabric Number	A/C Ratio (ft/min)	NH_3/NO_x Molar Ratio	NO_x Inlet (ppm)	NO_x Outlet (ppm)	NO_x Removal Efficiency (%)	Ammonia Slip (ppm)	SO_3 Conc. (ppm)	HCl Conc. (ppm)	Particulate Removal Efficiency (%)
				Washed, Illinois, #6 Bituminous					
2	2	0.9	540	58	89.3	5	2		
2	3	0.9	535	81	84.9	7	2	---	99.8
2	4	0.9	590	112	81.0	22	124		
13	2	1.1	673	34	94.9	64	4		
13	3	1.1	686	64	90.7	58	2	---	99.4
13	4	1.1	688	126	81.7	88	169		
				Jacobs Ranch, Wyoming, Subbituminous					
2	2	0.9	785	59	92.5				
2	3	0.9	760	75	90.1	86	<1	---	99.9
2	4	0.9	800	90	88.8				
13	2	0.9	645	80	87.6				
13	3	0.9	680	105	84.6	99	<1	---	99.9
13	4	0.9	675	195	71.1				
				South Hallsville, Texas, Lignite					
2	3	0.9	900	175	80.6	121	1	17	----
13	2	0.9	820	110	86.6				
13	3	0.9	810	145	82.7	75	1	<1	99.8
13	4	0.9	825	195	76.4				
				Pyro Kentucky Bituminous					
2	2	0.9	970	93	90.4				
2	3	0.9	930	130	86.0	10	1	---	99.7
2	4	0.9	925	178	80.8				
13	3	0.9	810	170	79.0	30	1	142	96.6

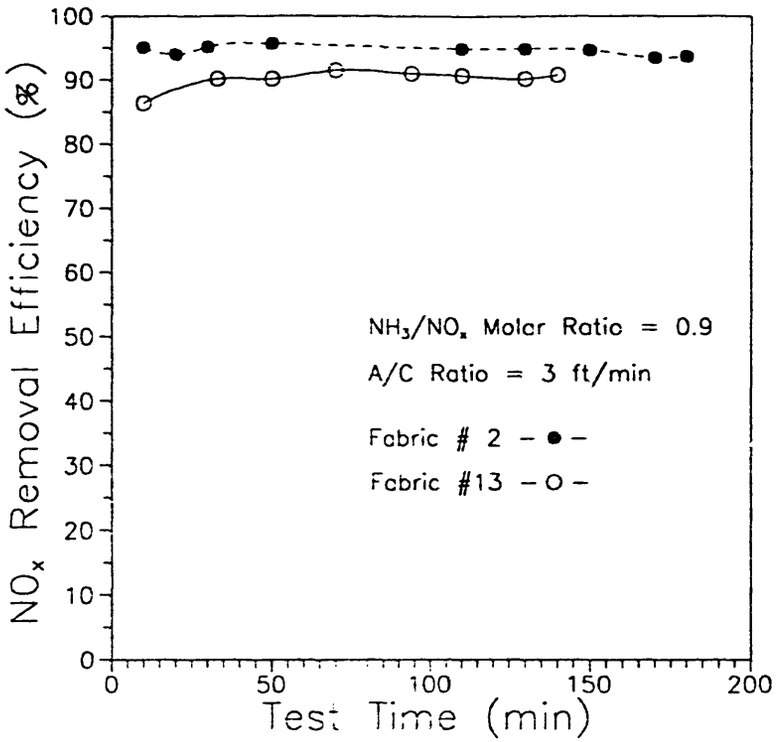

Figure 2. NO_x removal efficiency as a function of time, fabric, and air-to-cloth ratio for a washed Illinois #6 biuminous coal.

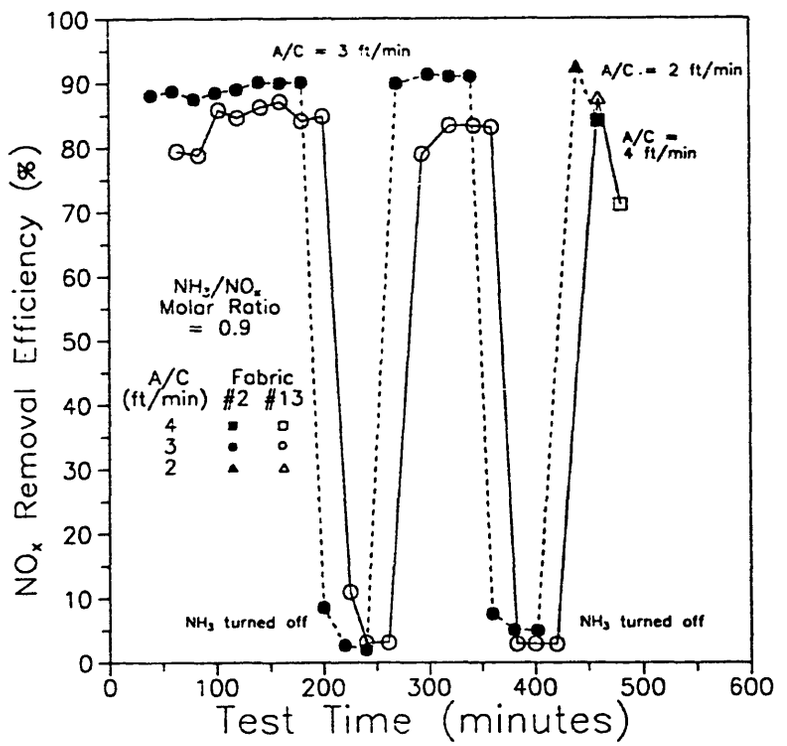

Figure 3. NO_x removal efficiency as a function of time, fabric, and air-to-cloth ratio for a Jacobs Ranch subbituminous coal.

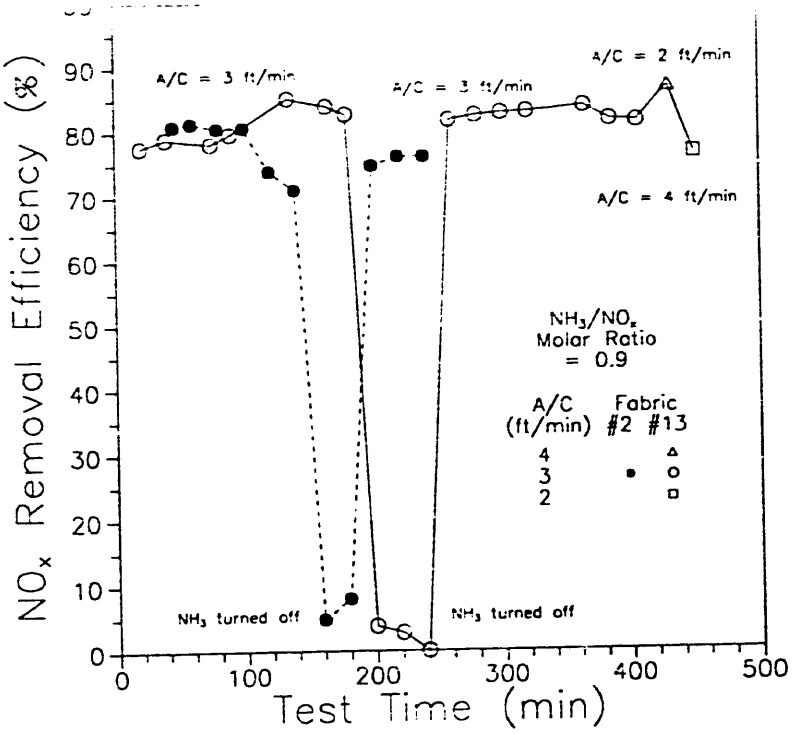

Figure 4. NO_x removal efficiency as a function of time, fabric, and air-to-cloth ratio for a South Hallsville, Texas, lignite.

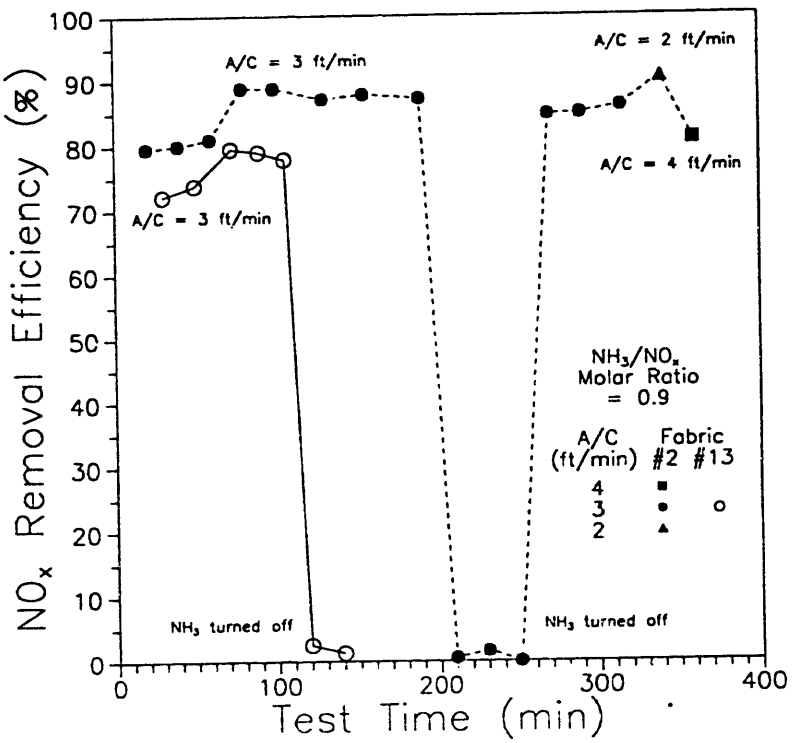

Figure 5. NO_x removal efficiency as a function of time, fabric, and air-to-cloth ratio for a pyro Kentucky bituminous coal.

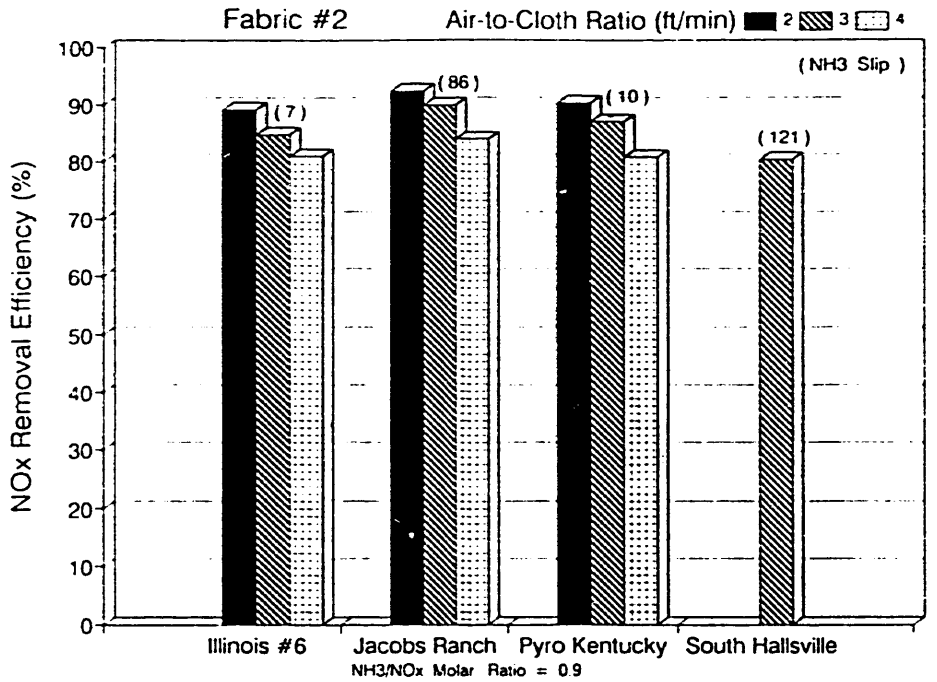

Figure 6. Comparison of the catalytic performance using four different coals for fabric #2.

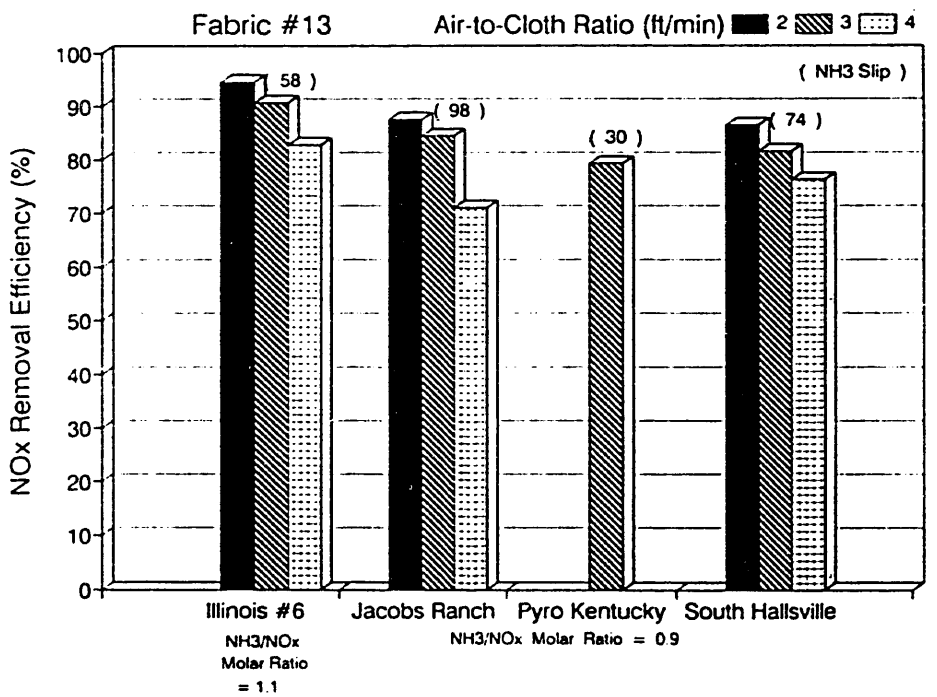

Figure 7. Comparison of the catalytic performance using four different coals for fabric #13.

As was expected, the HCl concentration in the flue gas during the tests using Pyro Kentucky bituminous coal was high, 142 ppm. The calculated value for a coal with a chlorine content of 0.2% burned in the EERC PTC is 149 ppm. In addition, two HCl measurements were made during the tests burning the South Hallsville, Texas, lignite, which has essentially zero chlorine content. The first test using fabric #2 verified this, as the measured concentration was <1 ppm. However, the HCl concentration in the flue gas for the second South Hallsville test using fabric #13 was 17 ppm. This test was completed following a Pyro Kentucky test, and therefore the higher HCl value may have been a result of residual HCl absorbed on fly ash adhering to the combustor wall or flue gas duct.

As is shown in Figure 6, it appears that NO_x removal efficiency with fabric #2 was similar (85% to 90%) for three of the four coals fired in the pilot-scale combustor. The exception was observed when firing the South Hallsville, Texas, lignite. Although an obvious explanation for this result (80% NO_x removal efficiency and 121 ppm ammonia slip) is not apparent, EERC believes that the filtration characteristics of the South Hallsville fly ash may have contributed to the observed result. Specifically, South Hallsville, Texas, lignite is known to produce an ash difficult to collect in a fabric filter (1). A large number of pinholes was present in the dust cake at the conclusion of the test. Pinholes may result in localized areas of very high air-to-cloth ratios which, depending on the number and size of the pinholes, can limit contact between the flue gas and the catalyst, resulting in decreased NOx removal efficiency.

For fabric #13 (shown in Figure 7) the results using South Hallsville, Texas, lignite were more successful as excessive pinholing did not occur. However, the NO_x removal efficiency was somewhat lower, about 83% compared to 86% and 90% for the Jacobs Ranch and Illinois #6 coals, respectively, again indicating that some coals appear to have an effect on catalyst-coated fabric performance. The results using the Pyro Kentucky bituminous coal with fabric #13 are suspect due to an upset in the pilot-scale combustion system. Excessive slagging resulted in an unstable flame in the burner, causing an early shutdown of the test.

Figures 2 through 5 compare the NOx removal efficiency as a function of time for fabrics #2 and #13 while firing the four different coals. With the possible exception of the South Hallsville, Texas, lignite (Figure 4), the NO_x removal efficiency was geater for fabric #2 than for fabric #13.

Surface area and vanadium concentrations were determined for each of the fabrics tested. The surface area was measured using a BET monosorb surface area analyzer. The vanadium concentration on the fabric was determined by first weighing a small amount of the catalyst-coated fabric, and then dissolving it in a solution of ultrapure hydrofluoric acid followed by a solution of ultrapure aqua regia. The liquid was then diluted to 100 mL with deionized water and analyzed for vanadium using atomic absorption techniques.

Table 3 presents the surface area and vanadium concentration data for each of the fabrics tested. Both were measured prior to exposure to the flue

gas and after completion of the reactivity tests. In all cases, exposure of the fabric samples to flue gas resulted in a substantial decrease in surface area. Although the vanadium concentration on the fabric did tend to show a decrease after exposure to flue gas, for several of the fabrics (#2, #5, #14), the change was essentially zero. Figure 8 shows surface area as a function of vanadium concentration for both the exposed and unexposed fabrics. The two plots are anchored at the theoretical surface area calculated for a blank fabric. Both the graph and table tend to support the conclusion that a large percentage of the catalyst pore structure was located at or near the surface. During use, some of the catalyst sluffs off at the surface, resulting in a greater percentage decrease in surface area.

BET surface area data for the fabric samples exposed to flue gas are plotted as a function of ammonia slip in Figure 9. The figure includes data from Task A, as presented in the previous annual report (2). Task B data only included the fabrics that were tested at an ammonia/NO_x molar ratio of 0.9 and at an air-to-cloth ratio of 2 ft/min, so that comparisons can be made to Task A results. Although there is some data scatter, the conclusions that were made previously appear to be valid. Fabric samples having a surface area of 6 to 9 m^2/g resulted in low ammonia slip (<10 ppm). Surface area values between 4 and 6 m^2/g resulted in moderate ammonia slip (10 to 50 ppm). Below 4 m^2/g, the ammonia slip values increased exponentially.

Although other factors such as weave texturization may also be important, Figure 10 shows that the concentration of catalyst on the fabric and the available surface area are directly proportional to NO_x removal efficiency. It is unclear as to why the surface area was so low for fabric #7 in relationship to the NO_x removal efficiency, as this was not the case when vanadium concentration was plotted as a function of NO_x removal efficiency.

Table 3 shows that two different samples of fabrics #2 and #13 were used in Task B. The first fabric samples were used to complete the fabric screening tests while firing the Illinois #6 coal and tests with the Jacobs Ranch subbituminous coal. However, after completing the two tests with the Jacobs Ranch coal, the fabrics were no longer usable due to excessive fraying. It was then necessary to obtain new fabric samples from Owens-Corning Fiberglas. There was a measurable difference in catalyst concentration between the first and second fabric samples. However, after the fabrics had been exposed to flue gas, the surface areas were similar. The issue of quality control, with respect to the coating process, has not been specifically addressed in any of the work completed by EERC. A joint review of the recent data by EERC and Owens-Corning Fiberglas would be appropriate, with respect to coating process and quality control issues.

3.2 Task E - Fine Particulate Characterization

Work was completed this past quarter in three areas in support of Task E. Extensive testing was completed with the Cohetester instrument, which provides a direct measurement of the tensile strength of a bulk powder such as fly ash. Testing was also completed with a Powder Characteristics Tester to determine aerated and bulk porosities for some fly ash samples, and initial

TABLE 3

VANADIUM CONCENTRATION AND BET SURFACE AREA
FOR EACH OF THE CATALYST-COATED FABRICS TESTED[a,b,c]

	Vanadium Concentration			BET Surface Area		
Fabric No.	Unexposed (mg/g)	Exposed (mg/g)	Change (%)	Unexposed (m^2/g)	Exposed (m^2/g)	Change (%)
Blank	0.03	---	---	0.56	---	---
2	9.1	9.0	1.1	9.50	6.19	34.8
2	8.4	8.3	1.2	10.68	5.11	52.2
3	4.7	3.7	21.3	3.31	1.54	53.5
4	4.7	4.2	10.6	4.28	2.02	52.8
5	5.5	5.4	1.8	5.79	3.74	35.4
7	7.6	6.3	17.1	6.62	2.74	58.6
13	6.8	6.1	10.3	5.76	4.04	29.9
13	8.4	8.0	4.8	6.52	4.00	38.7
14	3.4	3.6	-5.9	3.09	1.90	38.5
15	7.7	5.7	26.0	6.24	3.79	39.3

[a]Unexposed and exposed refer to exposure to flue gas.
[b]Vanadium concentration is expressed as mg vanadium per g of coated fabric.
[c]Fabric BET surface area is expressed as m^2 per g of coated fabric.

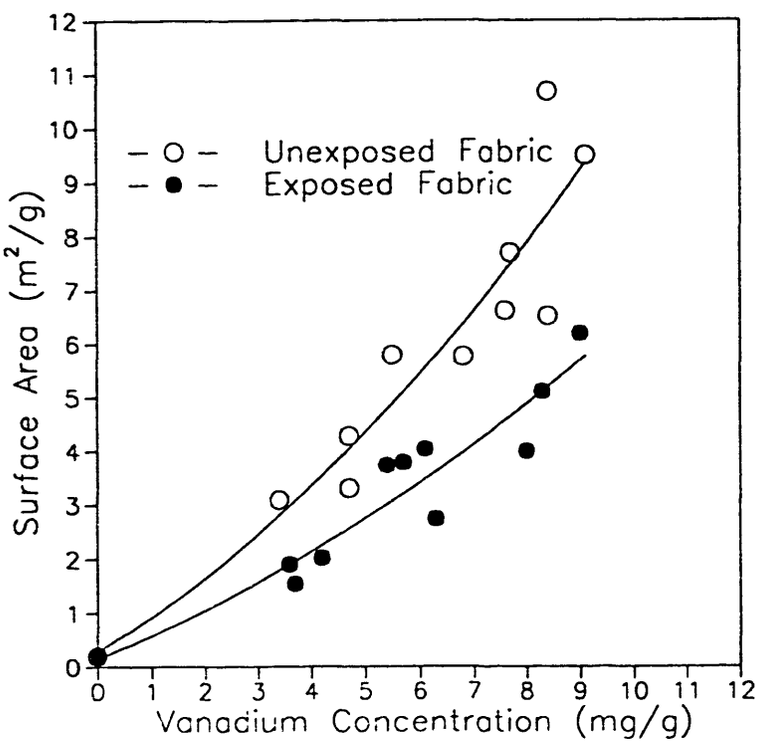

Figure 8. Vanadium concentration of both the exposed and unexposed catalytic fabrics as a function of surface area.

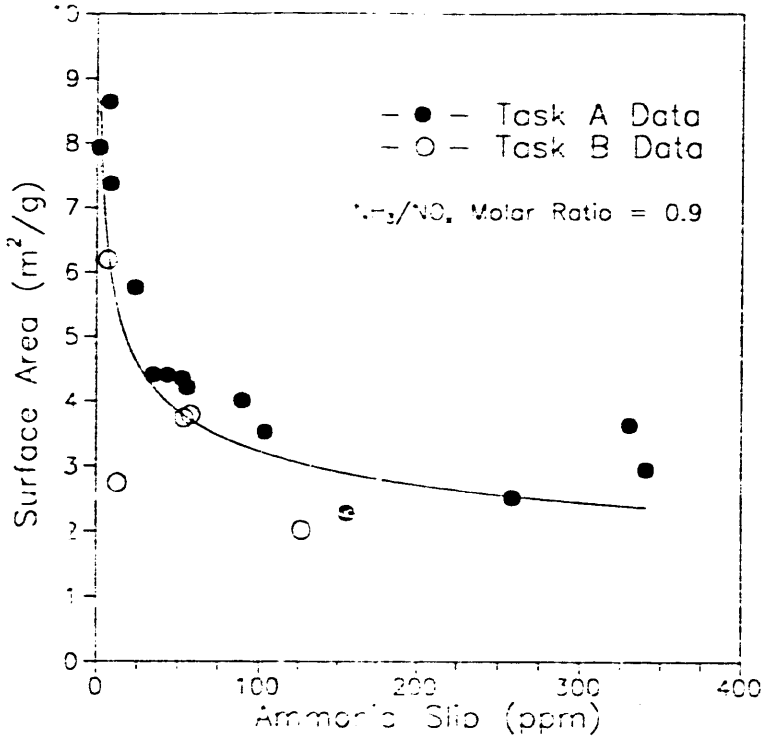

Figure 9. Surface area as a function of ammonia slip for both Task A and Task B results.

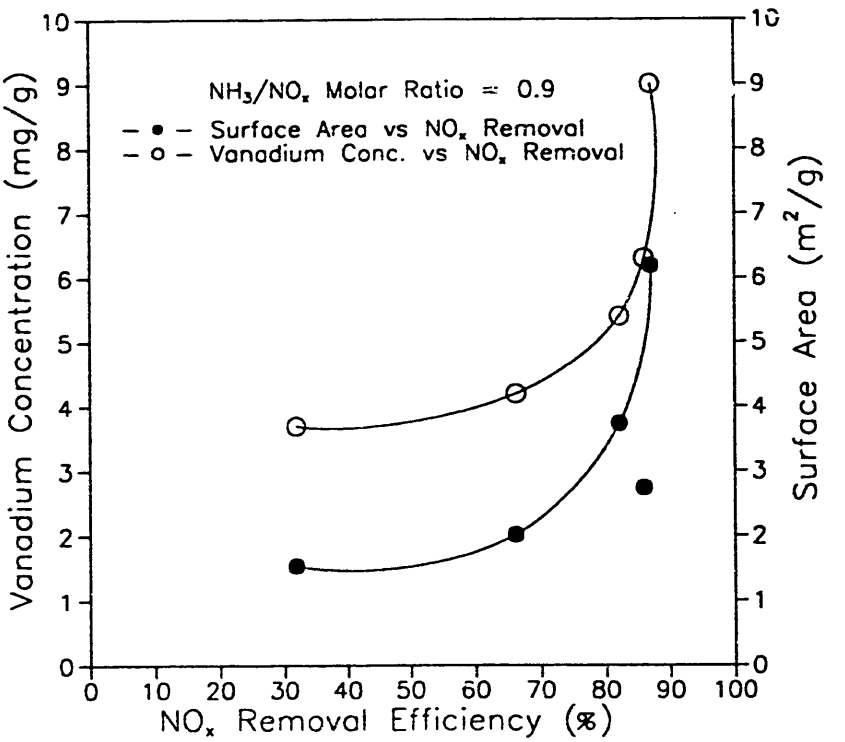

Figure 10. NO_x removal efficiency as a function of Vanadium concentration and surface area.

tests were completed with the recently constructed reentrainment device to measure K_2 for several dusts. Some of these results were presented in a paper entitled "Enhancing Baghouse Performance with Conditioning Agents: Basis, Developments, and Economics" by S.J. Miller and D.L. Laudal, at the Eighth EPA/EPRI Symposium on the Transfer and Utilization of Particulate Control Technology, which was held March 20-23, 1990, in San Diego, CA.

A schematic of the Cohetester is shown in Figure 11. The Cohetester measures the horizontal tensile force of the powder bed formed in the split cell consisting of 2 semicircles. There is no contact and thus no friction between the cell components during the testing sequence. An ash sample is placed in a 5-cm diameter cell split into two halves. One half of the cell is stationary, and the other half is suspended such that the cell can be pulled apart with minimal force when no powder is in the cell. When the powder bed is pulled, it is extended in the same direction as the tensile force. The Cohetester measures this displacement of the bed as well as the tensile force simultaneously, and the fracture curve is plotted on an X-Y recorder. Multiple tests at different compaction forces provide information to plot cohesive tensile strength as a function of porosity for a given ash. An example of the fracture curves is shown in Figure 12.

Cohetester tests were completed on previously collected fly ash samples, including those from tests in which ammonia and SO_3 were used as conditioning agents upstream of a baghouse and from tests without conditioning. Analysis of samples with the Cohetester should help to provide a better understanding of, and an explanation for, the reduced particulate emissions and baghouse pressure drop that occurred with conditioning. Three composite samples of baghouse hopper ash were previously collected during each 500-hour baseline and conditioning test with Monticello coal (one composite sample per week). Cohetester results with these six samples are shown in Figure 13. From these results we can conclude that conditioning significantly increased the cohesive tensile strength for a given porosity. The range in porosities was determined by the range in compaction force, which was the same for both conditioning and baseline tests. The maximum compaction force allowable with the Cohetester resulted in a porosity of 39% for the baseline samples and 53% for the conditioned tests. Similarly, the minimum compaction force resulted in a porosity of only 51% for the baseline samples, compared to 67% for the conditioned samples. These results showed that another effect of conditioning was to greatly reduce the packing tendency of the ash.

Cohetester results for conditioned and baseline ash samples from Pittsburgh No. 8 coal are shown in Figure 14. Again, the conditioned sample had a much greater tensile strength at the same porosity, and the baseline sample has a much greater tendency to pack. While the difference between conditioned and baseline samples was obvious, there was also a difference in the cohesive curves when the Pittsburgh No. 8 and Monticello samples were compared. At the maximum compaction force, the tensile strength for the Pittsburgh No. 8 was much lower. This comparison was more easily seen in Figure 15 where both sets of data are shown in addition to Cohetester results with a Beulah fly ash. An exponential curve is fit to each data set in Figure 15. As porosity approaches 100%, the tensile strength should approach zero. Interestingly, the conditioned Monticello and Pittsburgh No. 8 data form the same approximate exponential curve, indicating that, at the same porosity,

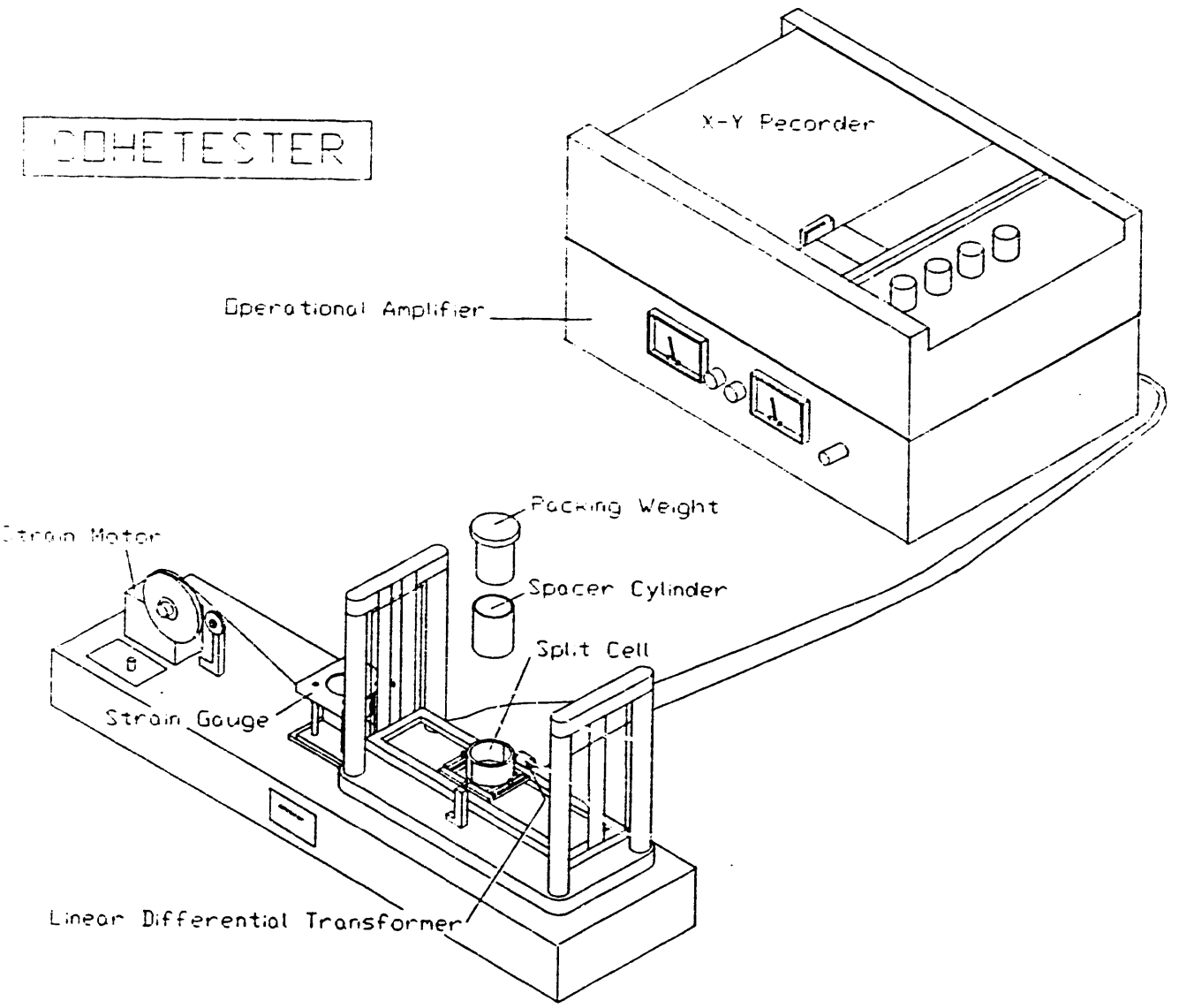

Figure 11. Schematic of the Cohetester.

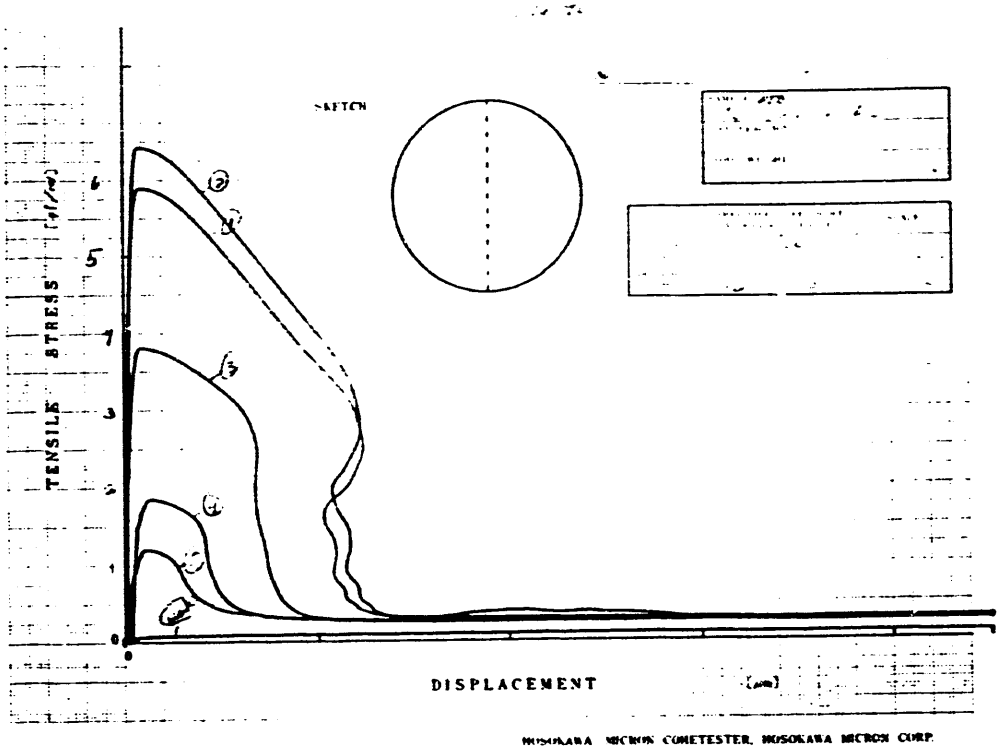

Figure 12. Example of fracture curves produced with the Cohetester showing tensile strength as a function of displacement for several levels of compaction.

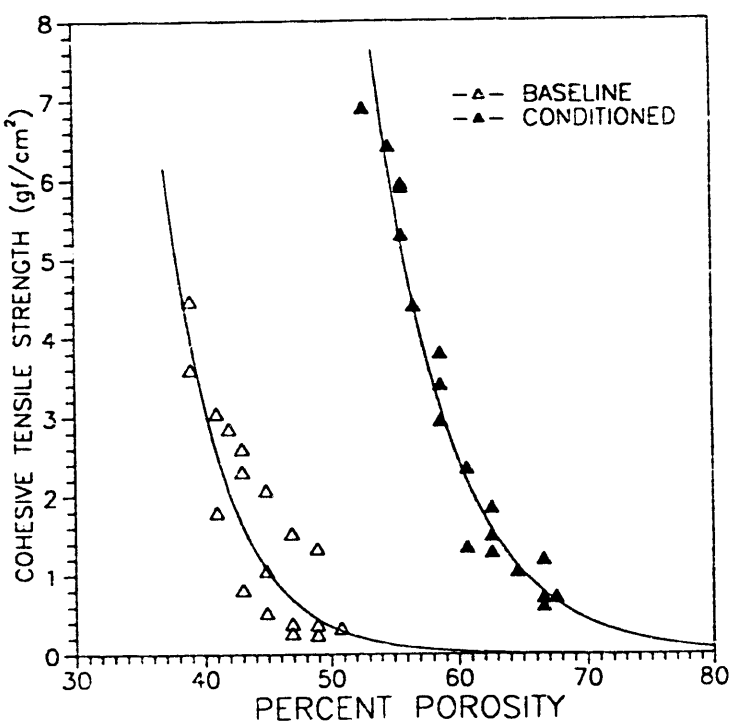

Figure 13. Cohesive tensile strength as a function of ash porosity for Monticello ash samples as measured by the Cohetester method.

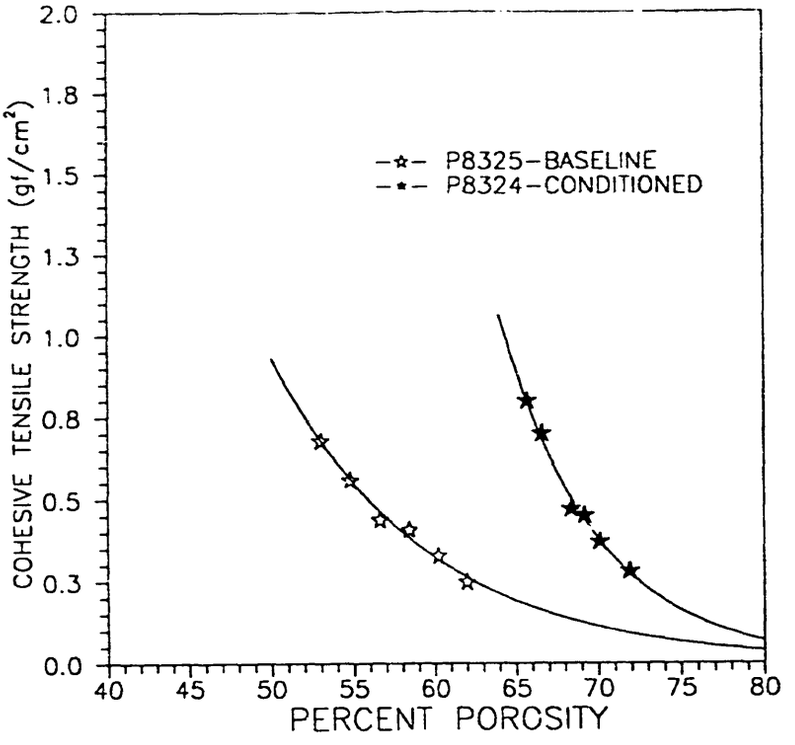

Figure 14. Cohesive tensile strength as a function of ash porosity for Pittsburgh No. 8 ash samples as measured by the Cohetester method.

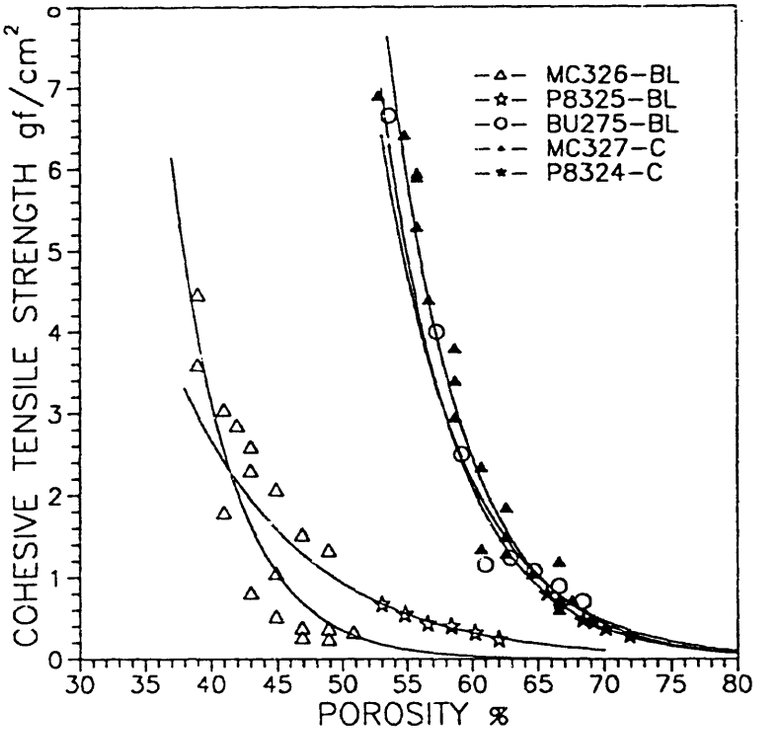

Figure 15. Cohesive tensile strength as a function of ash porosity for Pittsburgh No. 8, Monticello, and Beulah ash samples as measured by the Cohetester method. Exponential curves are fit to each data set.

they have the same tensile strength. However, the compaction force required to attain the same porosity value is different--the Monticello sample having a greater tendency to compact. Previously measured particle-size distributions for the Monticello and Pittsburgh ashes did not indicate any significant differences in particle sizes. Therefore, the explanation for the differences in behavior between the Monticello and Pittsburgh ashes is not clear. Other possible influences include the amount of surface moisture on the particle morphology. The Beulah ash sample (BU275) data closely followed the conditioned Monticello ash, in terms of covering the same porosity range and forming the same approximate exponential curve as the conditioned samples. The Beulah ash had not been conditioned, but in previous work had shown excellent collectibility characteristics. No conditioning experiments have been done with the Beulah ash, but an interesting question is whether conditioned Beulah ash would form a tensile strength-porosity curve to the right of the baseline curve.

Porosity characteristics of the baseline and conditioned ashes were also measured with a powder characteristics tester that performs several different mechanical measurements of bulk powder, such as fly ash (3). Two of the more useful measurements appear to be the aerated and packed density which, along with particle density, provide aerated and packed porosity. The aerated porosity is obtained by sifting an ash sample through a vibrating 60-mesh screen into a 100-cc cup, so that dust overflows the cup edge. The excess dust is scraped off with a knife edge and the weight of the known volume of dust is measured to determine the bulk density. The packed density is determined by adding an extension to the cup and filling the extension with additional sifted ash. The cup with the extension is then placed in a mechanism that raises the cup about 1/2 inch and lets the cup fall against a stop. This is done once per second for a period of 3 minutes. The cup extension is then removed and the excess dust scraped off as before. There is no external compaction force on the dust layer. Compaction is caused by the natural settling that occurs as the dust is shocked. Results of these tests are shown in Table 4 for the baseline and conditioned samples. Three or four repeat tests were completed on each of the three baseline and conditioned baghouse ash samples. Standard deviations shown in Table 4 include all baseline results grouped together and all conditioned results grouped together. Although there is slightly more data variation for the conditioned samples compared to the baseline samples, the effect of conditioning on the aerated and packed densities is very clear. These data again demonstrate that the baseline ash has a high tendency to compact and that conditioning imparts to the ash a resistance to packing. It would appear that dust cake porosity might be predicted by these measurements, but enough data are not available to correlate with actual dust cake porosity. In addition, actual dust cake porosity may depend on other factors such as face velocity, fabric type, and cleaning method. Nevertheless, the aerated and packed porosity measurements would appear to be useful methods in helping to predict baghouse pressure drop. However, further experimentation is needed to determine the effect of relative humidity on the absolute values of both packed and aerated porosities.

K_2 was measured for each of the three composite baghouse hopper ash samples for the baseline and conditioning tests. To determine K_2, a 150 g sample of ash was placed in the reentrainment cell, a cylinder with a porous bottom, and the pressure drop across the ash layer was measured at constant

TABLE 4

AERATED AND PACKED POROSITY [a,b]

Ash type	Aerated porosity (%)	σ	n	Packed porosity (%)	σ	n
Monticello baseline	62.6	0.6	9	40.1	0.8	9
Monticello conditioned	75.8	1.5	10	55.0	1.2	11

[a] σ = standard deviation
[b] n = number of tests

air flow rate through the dust for several levels of dust compaction. The porosity of the ash layer was calculated by measuring particle density by helium pycnometry and by measuring the dust layer thickness and cylinder diameter. Results of the K_2 measurements are shown in Figure 16, along with the Carman-Kozeny and Bush models that define K_2 in terms of porosity and particle size. The Carman-Kozeny relationship is derived from a theoretical capillary model and, assuming spherical particles, takes the form (4):

$$K_2 = 36\ k\ \mu\ (1 - \varepsilon) / \varepsilon^3\ P_p\ D^2 \qquad \text{Eq. 1}$$

where

K_2= specific dust cake resistance coefficient (sec/ft); note: K_2 can be converted to inches of water-ft-min/lb by multiplying by a factor of 311.6

k = Carman-Kozeny constant ($\tilde{=}5$) (dimensionless)
μ = gas viscosity (lb-sec/ft^2)
ε = porosity (dimensionless, void volume fraction)
P_p = particle density (lb/ft^3)
D^p = particle diameter (ft)

Bush et al. and Cushing et al. (5,6) have reported an empirical relationship between K_2 and porosity for coal fly ash:

$$K_2 = (4\ \mu / D^2\ \ P_p)\ [(1 - \varepsilon)/\varepsilon]\ [7.5 + 9.1(1 - \varepsilon) - 35.8(1 - \varepsilon)^2 + 560(1 - \varepsilon)^3] \qquad \text{Eq. 2}$$

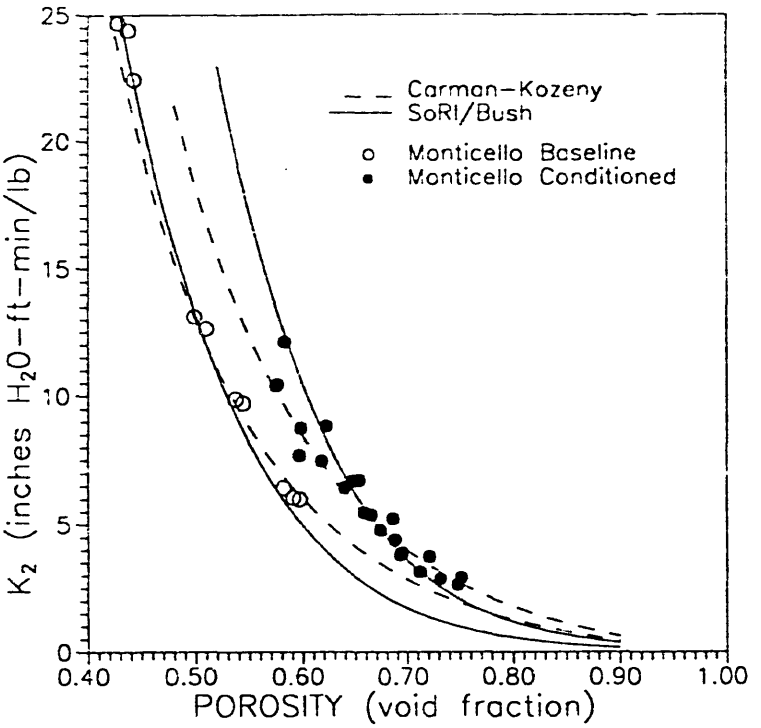

Figure 16. Specific dust cake resistance coefficient, K_2, as a function of ash porosity with Carman-Kozeny and SoRI/Bush models fit to data.

where the D term is referred to as the drag equivalent diameter. In the Carman-Kozeny equation, D refers to the actual physical diameter for monosized spheres. For fly ash with a broad particle-size distribution, the mass median diameter generally cannot be used for D for either equation. The value of the characteristic diameter is dependent on the particle-size distribution, specific surface area, and particle shape. These equations show that K_2 is most sensitive to particle size (or the characteristic particle-size term) and porosity. Any attempt, then, to alter K_2 should focus on these properties, and any explanation of a change in K_2 must include particle size and porosity. A curve for each of the models was fit to the measured K_2 and porosity values for both the baseline and conditioned data. It appears the baseline data follow both models closely, while the data from the conditioned test seem to more closely fit the Carman-Kozeny relationship. Both the baseline and conditioned results represent data from three separate samples. For a single sample, the K_2 measurements should define a smooth curve with minimal data scatter, as was the case for the individual samples. All data from the three baseline samples fit a nice curve with little variability. While the three conditioned samples showed more variability, their composite data still defined a distinct curve separate from the baseline data. The reason why the baseline and conditioned data formed separate curves is not clear. If the particle size distributions and the specific surface areas are unchanged, it is expected that the two data sets would define the same K_2 curve. Plausible explanations are that the particle-size distribution for the conditioned samples was somewhat smaller than the particle-size distribution for the baseline samples, or the conditioned samples had an increased specific surface area. Previous data have not clearly indicated any shift in the fly

ash particle-size distribution as a result of conditioning (7). Coulter Counter data did show the volumetric median diameter of one of the conditioned samples to be 11 μm compared to 13 μm for the baseline samples, but extensive data were not taken, and specific surface area measurements have not yet been completed.

The explanation why the baseline data in Figure 16 were over a porosity range of 43% to 60% (void fraction of 0.43 to 0.60), while the conditioned data covered a range of 58% to 75% is that the baseline ash had a much greater tendency to compact. Procedures were the same for all tests in that the same approximate compaction force was used to obtain the low porosity measurements, and no external compaction force was used to obtain the maximum porosity measurements. Ash porosity as a function of compaction force appears to be an important property of the dust which is also evident from other measurements.

Several important observations are obtained from the K_2 data and models in Figure 16. First, both the data and models demonstrated that a small increase in porosity can significantly reduce K_2. At constant dust cake weight and face velocity, this would correspond to a proportional decrease in baghouse pressure drop. Second, conditioning caused a distinct difference in the measured porosity range. These curves by themselves do not define the porosity of the baghouse dust cake, but it would appear to be a safe assumption that dust cake porosity for the baseline and conditioning tests would be somewhere between the respective minimum and maximum porosity values shown. The actual K_2 values of the dust cake during operation can be determined from dust loading and pressure drop data. The 500-hour tests were started with new bags, and the first 4 hours were conducted without bag cleaning. After the initial 4 hours, the tube sheet pressure drop was 10.5 inches of water for the baseline test and 2.15 inches of water for the conditioned test, which corresponds to a K_2 of 17 inches of water-ft-min/lb for the baseline test and 3.5 for the conditioned test. Looking at Figure 16, this implies that the dust cake porosity was about 47% for the baseline test and 71% for the conditioned test. K_2 can also be approximated by the increase in pressure drop between bag cleanings. From the 500-hour tests, pressure drop increased about 6.5 inches (from about 3 to 9.5 inches) between the 2-hour bag cleaning intervals for the baseline test, compared to about 1.4 inches (from about 0.8 to 2.2 inches) for the conditioning test. These data result in somewhat higher K_2 values of 21 for the baseline test corresponding to a dust cake porosity of 45% and 4.5 for the conditioned test corresponding to a dust cake porosity of 68%.

From the bench-scale and baghouse K_2 data, we concluded that the actual dust cake porosity for the baseline test was in the range of 45% to 47% and for the conditioned test in the range of 68% to 71%. Looking at the tensile strength values for these porosity ranges, an interesting result was observed. The corresponding tensile strength for the baseline tests was in the range of 0.7 to 1.0 g_f/cm^2 compared to 0.4 to 0.6 g_f/cm^2 for the conditioned tests. While there was some data scatter in this porosity range for the baseline tests and extrapolation of the conditioned data was necessary to obtain the tensile strength value for the highest porosity, the results indicated that the actual tensile strength of the dust cake decreased with conditioning, rather than increased. This result was not predictable because previous measurements of ash pellet strength (2) and effective angle of internal friction (7) showed that conditioning caused an increase in the

cohesive strength of the ash. However, this result was highly desirable because it would appear that bag cleanability would be directly related to the actual dust cake tensile strength. A reduction in dust cake tensile strength should facilitate bag cleaning. These results should be considered preliminary and need to be verified with other tests. The Cohetester tensile strength measurement, however, appears to be a good method to evaluate fly ash for fabric filter performance and possibly predict bag cleanability.

To summarize the effect of conditioning on baghouse pressure drop, several measurements showed a significant increase in ash porosity, which directly translates to increased dust cake porosity and reduced baghouse pressure drop. The conditioning has a double effect in that it increases porosity, which allows operation at a lower pressure drop. The lower pressure drop, in turn, reduces the compaction pressure on the dust layer, allowing a high porosity to be maintained. The reverse is true for the baseline ash or any ash that has a high tendency to compact. The tendency to compact causes high pressure drop, which results in a greater compaction force, leading to even lower porosity and higher pressure drop. Therefore, a treatment, such as ammonia and SO_3 conditioning that reduces the compaction tendency of the ash, can be effective in reducing baghouse pressure drop.

3.3 Project Budget and Milestones

The federal assistance Management Summary Report is presented as Tables 5 and 6. The report presents the budget information and milestone information through March 1990. In the previous quarterly reports for the current project year, a project budget of $200,000 was identified. Table 5 presents a project budget of $248,000. The $48,000 increase represents funds carried over from the previous project year. This carryover was planned and approved early in the current project year. The scope of work for the current project year was prepared assuming the $48,000 carryover would be available; therefore, no change in the current scope of work is planned at this time. Project milestones are on schedule at this time.

4.0 REFERENCES

1. Weber, G.F. and Laudal, D.L. "Final Technical Project Report for April 1988 through June 1989 for Flue Gas Cleanup." Work performed under DOE Contract No. DE-FC21-86MC10637, Grand Forks, ND, November 1989.

2. Miller, S.J. and Laudal, D.L. "Flue Gas Conditioning for Improved Fine Particle Capture in Fabric Filters: Comparative Technical and Economic Assessment." Vol II. Advanced Research and Technology Development, Low-Rank Coal Research Final Report, Work performed under DOE Contract No. DE-FC21-86MC10637, Grand Forks, ND, 1987.

3. Miller, S.J. "Flue Gas Conditioning for Fabric Filter Performance Improvement." Final Project Report for work performed under DOE Contract No. DE-AC22-88PC88866 for Pittsburgh Energy Technology Center, December 1989.

4. Scheidegger, A.E. The Physics of Flow Through A Porous Media. New York: The MacMillian Co., 1957.

5. Bush, P.V., Snyder, T.R., and Smith, W.B. "Filtration Properties of Fly Ash from Fluidized-Bed Combustion." J. of the Air Pollution Control Assn., 1987, 37: 1292.

6. Cushing, K.M., Bush, P.V., and Snyder, T.R. "Fabric Filter Testing at the TVA Atmospheric Fluidized-Bed Combustion (AFBC) Pilot Plant." EPRI CS-5837, May 1988.

7. Pohl, F.G. "A Novel Ring Shear Device for the Purpose of Classification of Fine Powders." Paper presented at the 17th Annual Meeting of the Fine Particle Society, San Francisco, CA, July 1986.

2.2 Waste Management

WASTE MANAGEMENT

Quarterly Technical Progress Report
for the Period January 1 through March 31, 1990

by

Charles J. Moretti, David J. Hassett,
Debra Pflughoeft-Hassett, Gale G. Mayer

University of North Dakota
Energy and Environmental Research Center
P.O. Box 8213, University Station
Grand Forks, North Dakota 58202

Contracting Officer's Technical Representative: Jerry Harness

for
United States Department of Energy
Office of Fossil Energy
Morgantown Energy Technology Center
Morgantown, West Virginia 26507

April 1990

Work Performed Under Cooperative Agreement No. DE-FC21-86MC10637

TABLE OF CONTENTS

LIST OF FIGURES

LIST OF TABLES

WASTE MANAGEMENT

1.0 GOALS AND OBJECTIVES

The objective of the Waste Management project is to characterize waste materials and by-products from advanced coal utilization processes, evaluate potential uses for these materials, and identify potential adverse environmental impacts associated with their use and/or disposal. Research is also being done to develop innovative waste management techniques for conventional and advanced coal utilization processes to comply with existing and/or future environmental regulations.

The activities of the Waste Management project include the following tasks:

Task 1. Activated Carbon Evaluation
Purpose - to evaluate the use of coal gasification char as activated carbon.

Task 2. Waste Characterization
Purpose - to characterize solid wastes from advanced coal utilization processes being developed at the Energy and Environmental Research Center (EERC).

Task 3. Coal Utilization Waste Conditioning Study
Purpose - to evaluate conditioning procedures for advanced coal utilization wastes.

Task 4. Bituminous Coal Fly Ash Data Collection and Evaluation
Purpose - to collect and evaluate data concerning the chemical and mineral compositions and physical properties of bituminous coal fly ash.

2.0 ACCOMPLISHMENTS

The following are the accomplishments of the Waste Management project for this reporting period:

2.1 Activated Carbon Evaluation

Limited testing of commercial activated carbons was performed during this period. A mild gasification lignite char was selected for further evaluation of activated carbon characteristics. Testing of the mild gasification chars will commence when they are made available.

2.2 Waste Characterization

Limited trace element characterization of the four bed materials submitted for this task was completed during this quarter. The trace element characterization included method development for an appropriate dissolution technique. Several initial dissolution techniques resulted in incomplete sample dissolution. The undissolved residues from these techniques were

submitted for scanning electron microscopy microprobe analysis. Results of this technique indicated the residues contained only calcium. The remaining trace element characterization will be completed on sample solutions generated from the original dissolution techniques.

Leachates generated from the EPA-EP toxicity leaching tests, toxicity characteristics leaching procedure (TCLP) and the synthetic groundwater leaching procedure (SGLP) short-term leaching tests were analyzed for trace constituents identified in the previous quarterly report. Leachates from the long-term leaching (LTL) tests were also analyzed for the same trace constituents. An additional set of long-term leaching experiments were initiated. Originally this set was planned as a four-week experiment. Results from the one-week LTL prompted re-evaluation of the second LTL experiments, and it was decided to extend the leaching time to three months.

2.3 Coal Utilization Waste Conditioning Study

During this reporting period, leaching tests were performed on advanced coal utilization wastes to study the effect of conditioning moisture on trace element leaching. The wastes studied included a composite cyclone ash and a baghouse fly ash from the Shawnee AFBC unit, an ESP fly ash from the Black Dog AFBC unit, and a Class C fly ash from a conventional cyclone-fired boiler.

Leaching test data from the Black Dog, TVA, and Riverside ashes, which had been conditioned with different moisture levels, were evaluated to determine the effect of conditioning moisture on trace element leaching. The test data indicated that selenium, chromium, barium, and molybdenum were the principally measured trace elements present in the ash leachates at environmentally significant concentrations. To illustrate the test results, plots were developed showing leachate trace element concentrations as a function of conditioning moisture levels. The plots showed that in several cases, a functional relationship appeared to exist between concentrations of some trace elements in the leachates and the moisture level used to condition the ash prior to compacting and curing.

2.4 Bituminous Coal Fly Ash Data Collection and Evaluation

During this quarter, groups having agreed to participate by providing the requested information and/or ash samples were sent an informational packet to facilitate their participation. A copy of the information request is included as Appendix A. The Edison Electric Institute Power Directory Data Base was received and reviewed for additional contacts for participation in the Coal Ash Data Base. The existing updated version of the Western Fly Ash Data Base was reviewed, and additional fields for inclusion of other data pertinent to bituminous coal ash were created.

Initial contacts continued throughout the quarter by mail and telephone to identify additional participants.

3.0 PROJECT RESULTS

3.1 Activated Carbon Evaluation

3.1.1 Introduction

No changes.

3.1.2 Research Scope

The objective of this research task has been modified due to changes in the scope of mild gasification. Testing will continue on the evaluation of chars from the mild gasification process and will be directed specifically toward characterization and evaluation of chars from the mild gasification of lignite.

3.1.3 Activated Carbon Evaluation Results

The hardness number is a measure of the resistance of a granular carbon to the effects of handling and carbon attrition. The GAC hardness number has no relation to the hardness scale used for plastics, metals, or minerals. It is used as a measurable characteristic of a carbon for comparison to other activated carbons.

Hardness numbers were calculated for Calgon F-300 and F-400 and for Hydrodarco 3000 and 4000 granular activated carbons that were subjected to the action of steel balls on a Ro-Tap machine (1). Table 1 summarizes results of hardness number determinations. The maximum hardness number is 100. "H" represents the hardness number, and "H_2" is a check on the accuracy of the test. Results obtained during hardness evaluations were all within 2% of the calculated values.

3.2 Waste Characterization

3.2.1 Introduction

Wastes from advanced coal utilization processes being developed at UNDEERC are characterized for the selection of appropriate waste management techniques and to identify any significant or unusual problems associated with the advanced process wastes. The characterization protocol determines the chemical and mineralogical composition, physical properties, and leaching behavior of the waste materials. The information obtained from the characterization studies can be used to assess the environmental impacts, handling properties, and utilization potential of the advanced process wastes.

3.2.2 Research Scope

The wastes to be characterized in this task will be obtained from ongoing coal utilization research at UNDEERC. Wastes considered for this task may include materials from the low-temperature coal gasifier and the circulating fluidized-bed combustor (CFBC). Emphasis for the waste characterization task for the current year is on limestone bed materials from the Hydrogen Production project.

TABLE 1

HARDNESS NUMBER DETERMINATIONS OF COMMERCIAL ACTIVATED CARBONS

	[A] Weight of Sample Loaded onto Hardness Pan (g)	[B] Weight of Sample Retained on Test Sieve (g)	[C] Weight of Sample Collected on Catch Pan (g)	H = (B/A)100	H_2 = (1-C/A)100
Calgon F-300	50.0	36.61	12.87	73.2	74.3
Calgon F-400	50.0	40.16	9.18	80.3	81.6
Hydrodarco 3000	50.0	32.78	16.52	65.6	67.0
Hydrodarco 4000	50.0	28.09	21.37	56.2	57.3

3.2.3 Waste Characterization Results

The physical properties, major chemical constituents, and the proton induced x-ray emission (PIXE) screening study results have been included in previous quarterly reports. Results from the initial limited trace element characterization are listed in Table 2. Temperatures and steam/carbon ratios are listed as identifiers for each bed material. All of these bed materials are limestone. For each of these four trials, Wyodak coal was used, and a reducing atmosphere was maintained.

Leaching results from the EPA-EP toxicity, TCLP, SGLP, and the one-week LTL experiments performed during the previous quarter are included as Appendix B.

3.3 Ash Conditioning Study

3.3.1 Introduction

Coal combustion wastes are usually conditioned prior to disposal by adding water. Conditioning helps to control dusting, increase the cohesiveness of the waste, and facilitate compacting at the disposal site. Previous research conducted at EERC has shown that, for self-hardening fly ashes, conditioning also initiates chemical reactions which increase the unconfined compressive strength of the compacted ash and reduce its hydraulic conductivity (1). These results suggest that appropriate conditioning of self-hardening ashes may affect their long-term environmental impact to a much greater extent than previously thought.

Wastes from advanced coal utilization processes, such as atmospheric fluidized-bed combustion (AFBC) and coal gasification, often display some

TABLE 2

TRACE CONSTITUENTS OF HYDROGEN PRODUCTION BED MATERIALS

	6-W380L	10R-W180L	12R-W275L	14-W170L
Temperature (Ave. °C)	801.70	806.36	749.95	698.59
Steam/Carbon (Ave.)	3.41	1.28	2.35	1.57
	(concentrations are µg/g)			
Barium	32	86	58	55
Boron	360	360	559	219
Chromium	7.2	26	8.6	11
Lead	0.7	1.7	2.3	1.2
Manganese	280	312	91	137
Titanium	62	384	91	137

degree of self-hardening behavior, particularly if they contain spent, calcium-based sorbents. Hardening occurs because free lime in the spent sorbent reacts with pozzolanic components of the ash to form interparticle bridges.

Since the amounts of waste produced from advanced coal utilization processes will increase as the advanced processes replace conventional processes, a research project is being conducted to optimize the conditioning process for advanced process wastes to reduce their long-term environmental impacts. The objective of the project is to determine the relation between conditioning moisture and the compacted dry density, unconfined compressive strength, permeability coefficient, and amounts of trace metals leached from several representative advanced process wastes. Additionally, a self-hardening fly ash from a conventional coal combustion process has been included in this study to determine whether conventional and advanced process wastes react to the conditioning process in a similar manner.

3.3.2 Materials and Methods

The advanced process wastes being studied include a composite cyclone ash and a baghouse fly ash from the Shawnee AFBC unit, an ESP fly ash from the Black Dog AFBC unit, and a spent bed material ash from the KRW fluidized-bed gasifier. All three wastes were produced from processes that used limestone addition to the bed for sulfur capture.

The AFBC units are both commercial scale plants. The Black Dog Plant is owned by Northern States Power Company; it has a 125-MW generating capacity and burns western subbituminous coal. The Shawnee Plant is owned by the Tennessee Valley Authority; it has a 160-MW generating capacity and burns bituminous coal. The KRW gasifier is a pilot-scale unit. It is being developed for integrated gasification combined cycle (IGCC) applications. The spent bed material being used for this study was obtained from a gasification run that used Pittsburgh #2 bituminous coal.

In addition to the three advanced process wastes, a self-hardening fly ash from a conventional cyclone-fired boiler burning a western subbituminous coal was included in this study. The fly ash was produced at the Riverside Plant owned by Northern States Power Company. This ash was included because it exhibits similar behavior in many respects to the AFBC ashes. If it is found that the behaviors of the Riverside fly ash and the advanced process wastes are fundamentally related, this will indicate that many techniques already developed for conditioning of conventional self-hardening fly ash can be successfully applied to some advanced process wastes.

The research plan for this project consists of an initial characterization task to establish baseline elemental composition, mineral composition, and physical property data for the coal combustion wastes. Moisture-density tests will be done to determine optimum moistures for maximum compacted dry densities. Unconfined compressive strength tests, permeability tests, and leaching tests will be done to determine how these important disposal-related properties vary as a function of the conditioning moisture level and how they relate to the optimum moisture (for maximum compacted density).

The moisture-density tests were performed by: (1) mixing each waste material with different amounts of water using a paddle type mixer, (2) allowing the mixtures to stand for 35 minutes and then remixing the material by hand, (3) preparing duplicate 1/30 ft^3 cylinders from each mix using standard Proctor compaction, and (4) measuring the dry density and moisture content of each cylinder.

The mixtures were allowed to stand for 35 minutes before compacting to allow them to hydrate and cool somewhat. Since it would take at least 35 minutes at a commercial plant to haul the conditioned waste to the disposal site and place it, this time interval was thought to be fairly representative of in-field disposal conditions.

The waste cylinders prepared for the moisture-density tests were cured for 28 days at 70°F and then tested for unconfined compressive strength and permeability coefficient. The unconfined compressive strength was measured by loading a cylinder to failure in a testing machine and calculating the unit stress. The permeability coefficient was measured by wrapping a cylinder in a rubber membrane, confining the specimen in a triaxial cell, and measuring the rate at which water flowed through the specimen using a pressure head of approximately 5 psi.

Finally, leaching tests were performed on the conditioned ashes. For these tests, fragments from the compressive strength tests were crushed and passed through a no. 16 sieve. Trace elements were then extracted from the sieved material using a generic leaching test developed at EERC (i.e., the

synthetic groundwater leaching procedure). Each leachate was analyzed for arsenic, barium, cadmium, chromium, lead, mercury, selenium, silver, boron, and molybdenum concentrations. The data thus generated was evaluated to determine whether a functional relationship existed between the moisture level used to condition the ash and the amounts of trace elements leached.

3.3.3 Experimental Results

The results of the leaching tests performed on the Black Dog, TVA, and Riverside ashes conditioned with different moisture levels are contained in Tables 3, 4, and 5 respectively. The tables also contain physical property test results for each ash. The leaching test results for selenium, barium, chromium, and molybdenum are plotted as a function of conditioning moisture content in Figures 1, 2, 3, and 4 respectively.

Based on the plots of the leaching data, several different types of functional relationships appear to exist between the leachate trace element concentrations and the conditioning moisture levels. In some cases, the added moisture and curing of the compacted ash specimens produced lower leachate trace element concentrations, while in a few cases, the added moisture actually produced higher trace element concentrations. In those cases where the leachate trace element concentrations were found to decrease when conditioning moisture was added, the data indicated that either the concentrations decreased continually as the moisture level increased or they reached some minimum value at an intermediate moisture addition level.

The results of the leaching studies generally suggest that moisture conditioning, compacting, and curing the ashes from both advanced and conventional coal utilization processes can affect their leaching behavior.

3.4 Bituminous Coal Fly Ash Data Collection and Evaluation

3.4.1 Introduction

The objectives of the coal fly ash research during the first year will be to identify and evaluate bituminous coal fly ash data. The effort for the second and third years of the project will be to collect and characterize samples of bituminous coal fly ash according to characterization protocols developed under the Western Fly Ash Research, Development, and Data Center and to expand the existing data base on western coal fly ashes to include information on bituminous coal fly ashes gained through this task.

3.4.2 Research Scope

Chemical, mineralogical, and physical characterization information on bituminous coal fly ashes from varying sources will be obtained and added to an existing coal fly ash data base currently containing information on over 500 western coal fly ashes. The information will be collected from voluntary participants who generate or market bituminous coal fly ash or other research groups having access to this type of information. If sources of information being sought are inadequate, the information will be supplemented by characterization of submitted samples at the EERC Coal By-Products Laboratory and the NDSU Chemistry Department.

The addition of this information to the current Western Fly Ash Data Base will facilitate basic understanding of the character of bituminous coal fly ash and the variability of the material. This information will be valuable in current and future coal ash research.

3.4.3 Bituminous Coal Fly Ash Data Collection and Evaluation Results

Pertinent information on coal fly ash identification, source, and characterization that is not included in the current coal fly ash data base has been identified for the Bituminous Coal Fly Ash Data Base. The data collection effort is ongoing.

4.0 REFERENCE

1. "Activated Carbon Evaluation and Selection;" ATOCHEM Inc. Reprinted from U.S. Environmental Protection Agency Technology Transfer, Process Design Manual for Carbon Adsorption; October 1973; EPA 625/1-71-002a.

TABLE 3

LEACHING TEST RESULTS FOR THE CONDITIONED BLACK DOG AFBC ASH

	Specimen No.					
	1	2	3	4	5	6
Conditioning Moisture Addition Level (% Dry Wt.)	0	28.1	31.9	36.0	41.9	44.1
Compacted Dry Density (lbs/cu.ft.)	NA	70.5	71.6	73.0	69.0	68.0
Unconfined Compressive Strength (PSI)	NA	177	234	330	366	229
Permeability Coefficient (cm/sec)	NA	1.7E-4	1.4E-6	2.9E-6	1.4E-6	1.2E-6
Leachate Arsenic Conc. (µg/l)	<2.0	<2.0	<2.0	<2.0	<2.0	<2.0
Leachate Barium Conc. (mg/l)	<0.02	0.28	0.26	0.23	0.23	0.25
Leachate Cadmium Conc. (mg/l)	<0.02	0.03	<0.02	<0.02	<0.02	<0.02
Leachate Chromium Conc. (mg/L)	<0.02	0.17	<0.02	0.08	0.08	0.13
Leachate Lead Conc. (µg/l)	<10	<10	<10	<10	<10	<10
Leachate Mercury Conc. (µg/L)	<0.6	<0.6	<0.6	<0.6	<0.6	<0.6
Leachate Selenium Conc. (µg/L)	6.8	<2.0	2.0	<2.0	<2.0	<2.0
Leachate Silver Conc. (µg/L)	<1.0	<1.0	<1.0	<1.0	<1.0	<1.0
Leachate Boron Conc. (mg/L)	<0.5	<0.5	<0.5	<0.5	<0.5	<0.5
Leachate Molybdenum Conc. (mg/l)	0.39	0.37	0.42	0.49	0.4	0.39

NA - Not Applicable

TABLE 4

LEACHING TEST RESULTS FOR THE CONDITIONED TVA DOG AFBC ASH

	Specimen No.					
	1	2	3	4	5	6
Conditioning Moisture Addition Level (% Dry Wt.)	0	17.0	26.4	29.8	34.6	39.2
Compacted Dry Density (lbs/cu.ft.)	NA	73.9	76.2	76.9	76.2	72.3
Unconfined Compressive Strength (PSI)	NA	213	328	366	320	227
Permeability Coefficient (cm/sec)	NA	1.1E-4	3.8E-5	1.8E-5	3.9E-6	2.0E-5
Leachate Arsenic Conc. (µg/L)	<2.0	<2.0	<2.0	<2.0	<2.0	<2.0
Leachate Barium Conc. (mg/L)	0.2	0.22	0.22	0.20	0.20	0.20
Leachate Cadmium Conc. (mg/L)	<0.02	0.03	0.03	<0.02	<0.02	<0.02
Leachate Chromium Conc. (mg/L)	0.14	<0.02	0.12	0.08	0.08	0.12
Leachate Lead Conc. (µg/L)	<10	<10	<10	<10	<10	<10
Leachate Mercury Conc. (µg/L)	<0.6	<0.6	<0.6	<0.6	<0.6	<0.6
Leachate Selenium Conc. (µg/L)	8.5	3.8	4.5	2.9	2.9	2.5
Leachate Silver Conc. (µg/L)	<1.0	<1.0	<1.0	<1.0	<1.0	<1.0
Leachate Boron Conc. (mg/L)	<0.5	<0.5	<0.5	<0.5	<0.5	<0.5
Leachate Molybdenum Conc. (mg/L)	0.17	0.14	0.24	0.11	0.11	0.20

NA - Not Applicable

TABLE 5

LEACHING TEST RESULTS FOR THE CONDITIONED RIVERSIDE FLY ASH

	Specimen No.					
	1	2	3	4	5	6
Conditioning Moisture Addition Level (% Dry Wt.)	0	4.1	5.1	8.9	10.6	12.6
Compacted Dry Density (lbs/cu.ft.)	NA	94.1	88.5	86.2	87.1	82.6
Unconfined Compressive Strength (PSI)	NA	231	334	405	401	387
Permeability Coefficient (cm/sec)	NA	2.7E-5	ND	1.7E-5	3.8E-5	9.4E-5
Leachate Arsenic Conc. (µg/L)	<2.0	<2.0	<2.0	<2.0	<2.0	<2.0
Leachate Barium Conc. (mg/L)	0.91	0.73	0.37	0.46	0.28	0.08
Leachate Cadmium Conc. (mg/L)	<0.02	<0.02	<0.02	<0.02	<0.02	<0.02
Leachate Chromium Conc. (mg/L)	0.31	0.20	0.28	0.27	0.30	0.33
Leachate Lead Conc. (µg/L)	<10	<10	<10	<10	<10	<10
Leachate Mercury Conc. (µg/L)	<0.6	<0.6	<0.6	<0.6	<0.6	<0.6
Leachate Selenium Conc. (µg/L)	55.0	55.0	49.0	50.0	48.0	64.0
Leachate Silver Conc. (µg/L)	<1.0	<1.0	<1.0	<1.0	<1.0	<1.0
Leachate Boron Conc. (mg/L)	<0.5	<0.5	<0.5	<0.5	<0.5	<0.5
Leachate Molybdenum Conc. (mg/L)	0.79	0.49	0.60	0.52	0.49	0.46

NA - Not Applicable
ND - Data Not Available

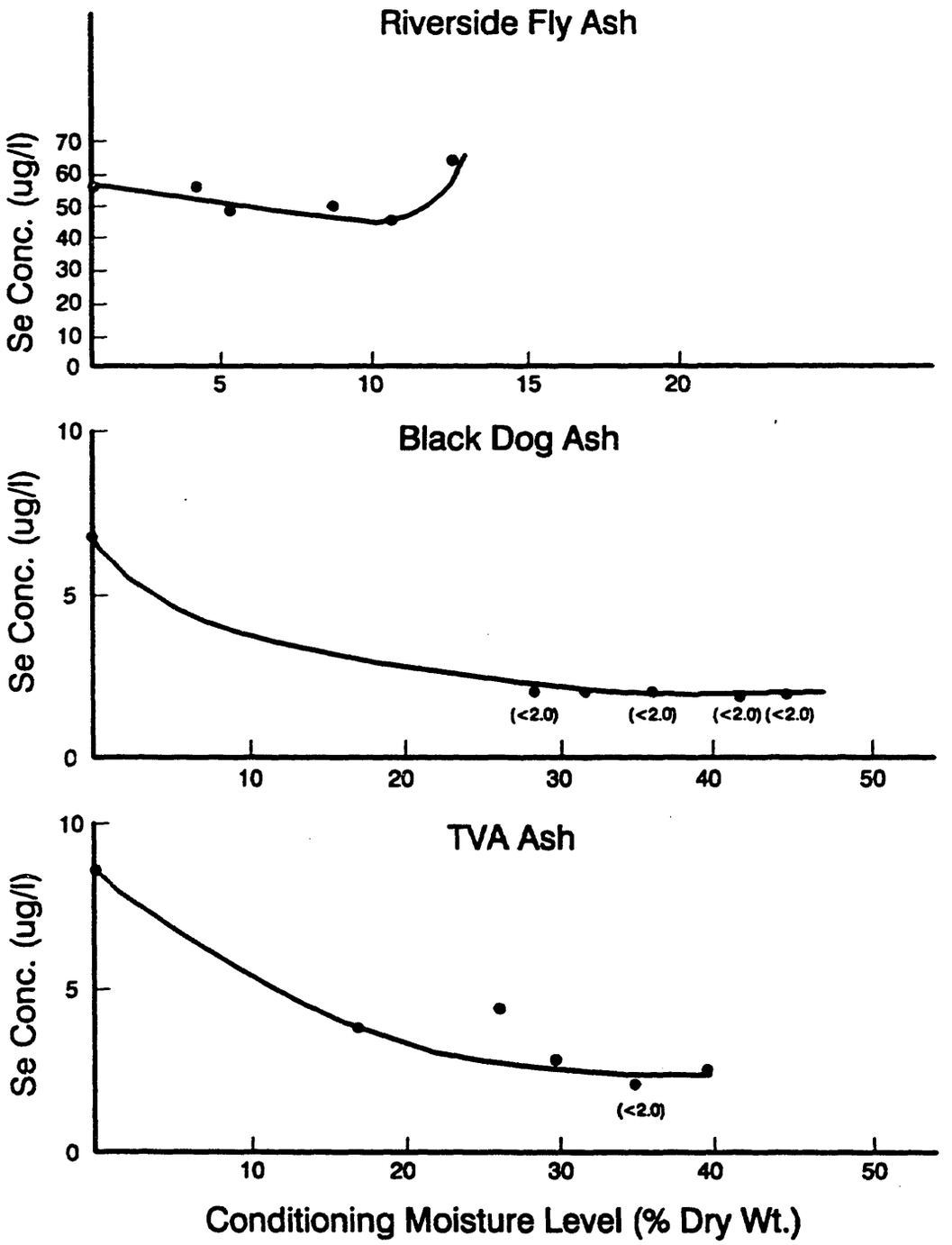

Figure 1. Leachate selenium concentration vs. conditioning moisture level for the Riverside, Black Dog, and TVA ashes.

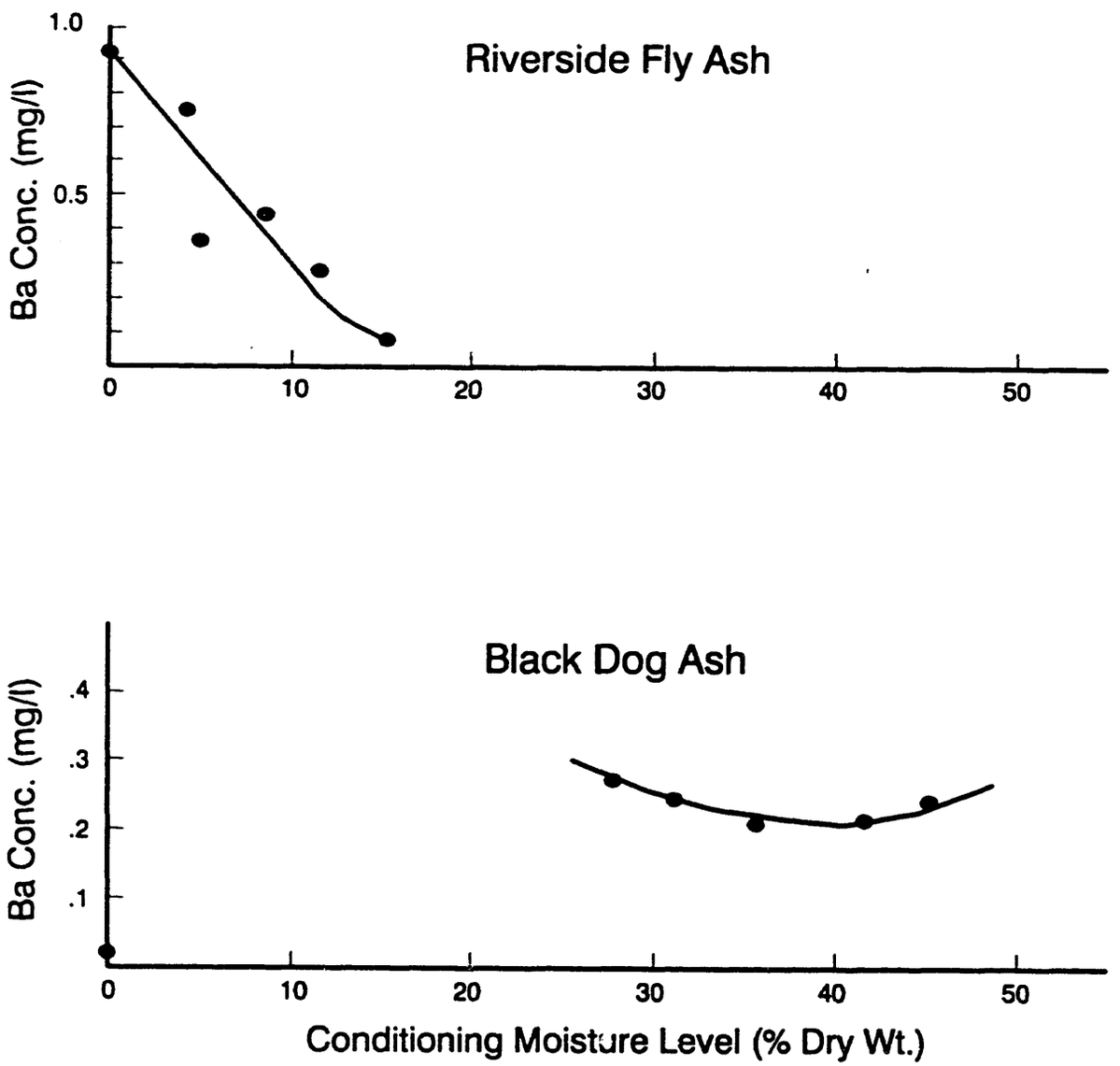

Figure 2. Leachate barium concentration vs. conditioning moisture level for the Riverside and Black Dog ashes. TVA graph showed negligible data.

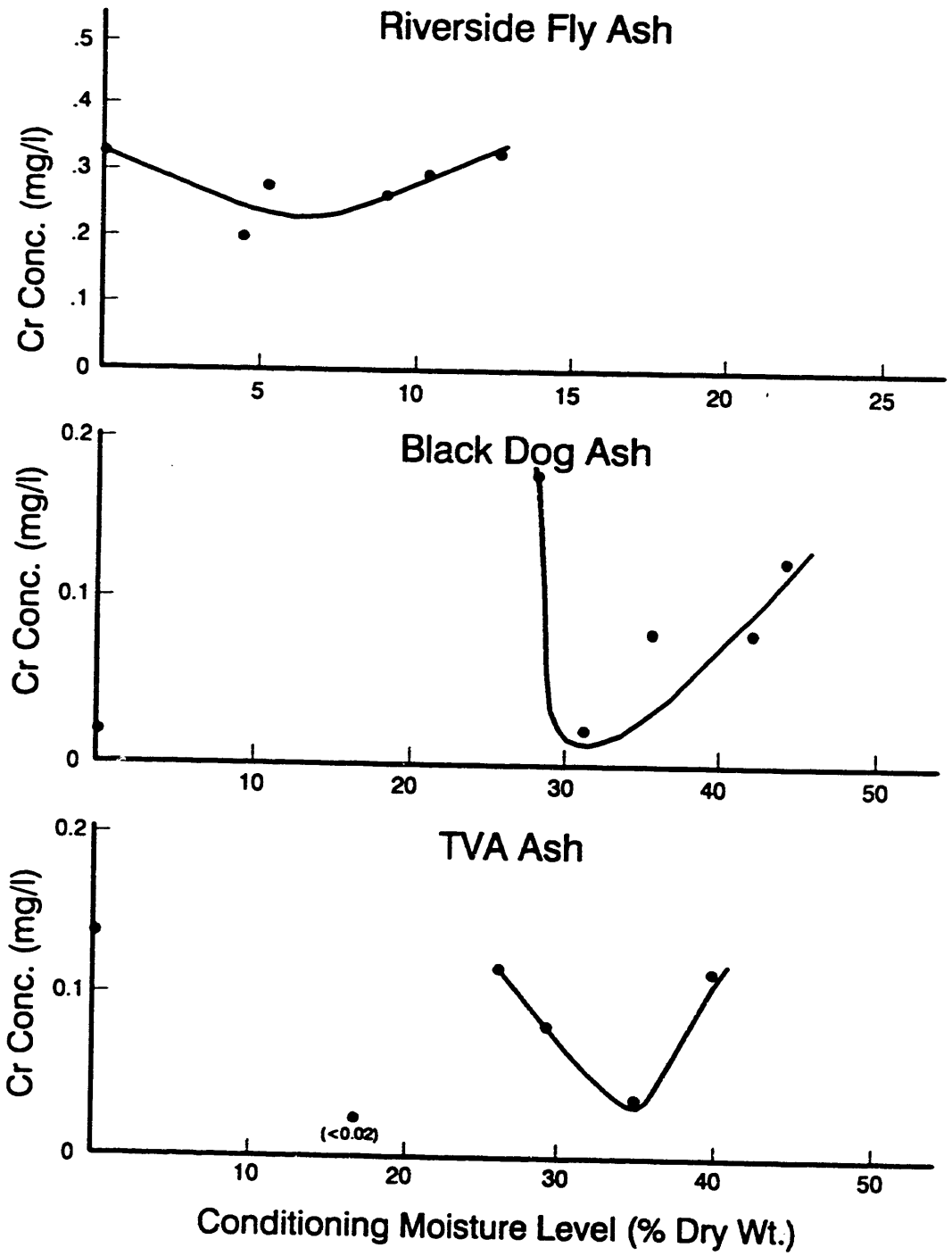

Figure 3. Leachate chromium concentration vs. conditioning moisture level for the Riverside, Black Dog, and TVA ashes.

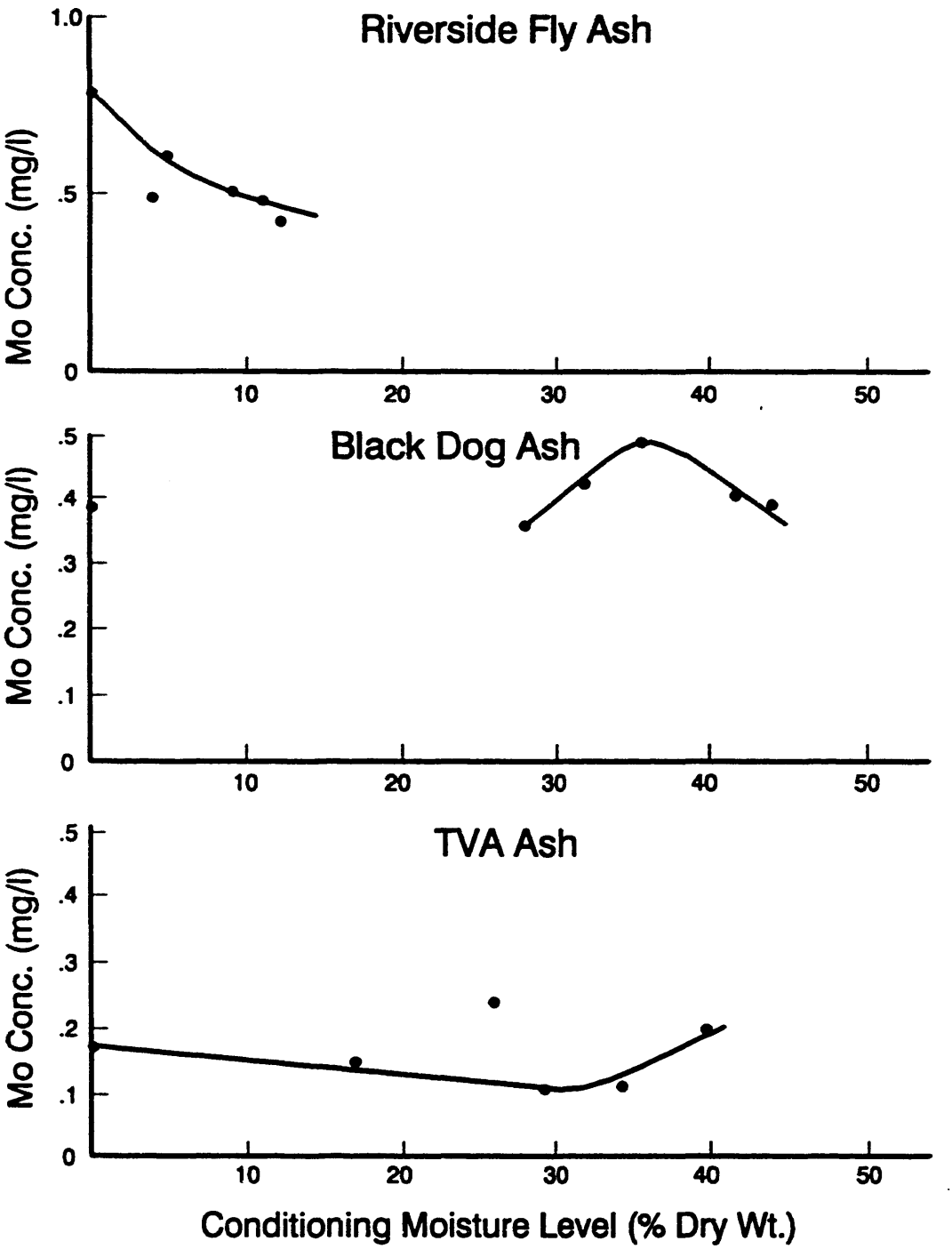

Figure 4. Leachate molybdenum concentration vs. conditioning moisture level for the Riverside, Black Dog, and TVA ashes.

APPENDIX A

APPENDIX A

INFORMATION FOR INCLUSION IN THE BITUMINOUS COAL ASH DATA BASE

Requested by University of North Dakota Energy and Environmental Research Center for a research project funded through the U.S. Department of Energy. Your voluntary participation is appreciated.

Source Information (This information will be coded in the data base to ensure anonymity of participants.)

1. Name of power company
2. Name of plant
3. Location of plant
4. Coal source
5. Boiler type
6. Boiler manufacturer
7. Source of ash (if handled by party other than the power company)
8. Collection method
9. Other information the participant finds pertinent and that is essential to identification or characterization of the ash

Chemical Composition (ASTM C618) or Other Analyses (e.g., XRD, ICAP, etc.)

1. Silicon dioxide (wt% SiO_2)
2. Aluminum oxide (wt% Al_2O_3)
3. Iron oxide (wt% Fe_2O_3)
4. Sulfur trioxide (wt% SO_3)
5. Calcium oxide (wt% CaO)
6. Magnesium oxide (wt% MgO)
7. Moisture content (wt% at 105°C)
8. Loss on ignition (wt% LOI at 750°C)
9. Available alkali (wt% Na_2O)
10. Sodium oxide (wt% Na_2O)
11. Potassium oxide (wt% K_2O)
12. Other major, minor, or trace elements such as As, Se, Ti, etc.
13. Leaching results on the ash such as EPA-EP tox, TCLP, ASTM, or other leaching tests

Physical Test Results (ASTM C618)

1. Fineness (% retained on 325-mesh sieve)
2. Pozzolanic Activity Index with Portland cement (%, ratio to control at 28 days)
3. Pozzolanic Activity Index with lime (psi, at 7 days)
4. Water requirement (% of control)
5. Soundness/autoclave expansion (%)
6. Specific gravity
7. Other parameters (slag viscosity, melting point, etc.)

Mineralogical Data

1. Mineralogical phases
2. Quantitative phase analysis
3. Other spectral information such as infrared or laser raman

APPENDIX B

ANALYTICAL RESULTS ON TASK 2 BED MATERIAL LEACHATES

	TCLP LEACHING			
	6-W380L	10R-W180L	12R-W275L	14-W170L
Aluminum	0.48	0.59	0.70	0.72
Arsenic	<5.0	<5.0	<5.0	<5.0
Boron	0.56	1.12	0.13	0.10
Cadmium	<0.02	<0.02	<0.02	<0.02
Calcium	2690	2630	2470	2290
Chromium	<0.1	<0.02	<0.1	<0.1
Copper	<0.2	<0.2	<0.2	<0.2
Iron	1.0	1.0	0.98	0.98
Lead	<0.5	<0.5	<0.5	<0.5
Magnesium	<0.1	<0.1	<0.1	<0.1
Manganese	<0.02	<0.02	<0.02	<0.02
Mercury	<3.0	<3.0	<3.0	<3.0
Molybdenum	<0.1	<0.1	<0.1	<0.1
Nickel	<0.1	<0.1	<0.1	<0.1
Phosphorous	<0.5	<0.5	<0.5	<0.5
Potassium	0.9	0.7	1.1	1.4
Selenium	<5.0	<5.0	<5.0	<5.0
Silicon	1.7	1.8	1.9	1.9
Silver	<0.2	<0.2	<0.2	<0.2
Sodium	3.0	6.3	2.4	7.0
Strontium	14.0	15.0	3.2	3.3
Titanium	<0.2	<0.2	<0.2	<0.2
Zinc	<0.1	<0.1	<0.1	<0.1
Zirconium	<0.1	<0.1	<0.1	<0.1

ANALYTICAL RESULTS ON TASK 2 BED MATERIAL LEACHATES

	EP-TOX LEACHING			
	6-W38OL	10R-W18OL	12R-W275L	14-W17CL
Aluminum	0.54	0.68	0.63	1.7
Arsenic	<5.0	<5.0	<5.0	<5.0
Boron	0.50	0.92	0.24	0.07
Cadmium	<0.02	<0.02	<0.02	<0.02
Calcium	2690	2650	2600	2360
Chromium	<0.1	<0.1	<0.1	<0.1
Copper	<0.2	<0.2	<0.2	<0.2
Iron	1.0	1.0	1.0	0.93
Lead	<0.5	<0.5	<0.5	<0.5
Magnesium	<0.1	<0.1	<0.1	<0.1
Manganese	<0.02	<0.02	<0.02	<0.02
Mercury	<3.0	<3.0	<3.0	<3.0
Molybdenum	<0.1	<0.1	<0.1	<0.1
Nickel	<0.1	<0.1	<0.1	<0.1
Phosphorous	<0.5	<0.5	<0.5	<0.5
Potassium	1.0	0.7	0.9	1.6
Selenium	<5.0	<5.0	<5.0	<5.0
Silicon	1.7	1.7	2.1	2.3
Silver	<0.2	<0.2	<0.2	<0.2
Sodium	2.6	5.4	2.1	6.6
Strontium	14	15	3.2	3.3
Titanium	<0.2	<0.2	<0.2	<0.2
Zinc	<0.1	<0.1	<0.1	<0.1
Zirconium	<0.1	<0.1	<0.1	<0.1

ANALYTICAL RESULTS ON TASK 2 BED MATERIAL LEACHATES

	SGLP 18 HR			
	6-W380L	10R-W180L	12R-W275L	14-W170L
Aluminum	0.26	0.35	0.30	0.32
Arsenic	<5.0	<5.0	<5.0	<5.0
Boron	0.46	0.98	0.17	0.45
Cadmium	<0.02	<0.02	<0.02	<0.02
Calcium	950	955	945	960
Chromium	<0.1	<0.02	<0.1	<0.1
Copper	<0.2	<0.2	<0.2.	<0.2
Iron	0.44	0.44	0.45	0.45
Lead	<0.5	<0.5	<0.5	<0.5
Magnesium	<0.1	<0.1	<0.1	<0.1
Manganese	<0.02	<0.02	<0.02	<0.02
Mercury	<3.0	<3.0	<3.0	<3.0
Molybdenum	<0.1	<0.1	<0.1	<0.1
Nickel	<0.1	<0.1	<0.1	<0.1
Phosphorous	<0.5	<0.5	<0.5	<0.5
Potassium	1.0	0.7	1.7	5.6
Selenium	<5.0	<5.0	<5.0	<5.0
Silicon	0.99	0.98	1.0	1.0
Silver	<0.2	<0.2	<0.2	<0.2
Sodium	2.4	5.7	1.7	5.6
Strontium	14.0	15.0	1.3	1.5
Titanium	<0.2	<0.2	<0.2	<0.2
Zinc	<0.1	<0.1	<0.1	<0.1
Zirconium	<0.1	<0.1	<0.1	<0.1

ANALYTICAL RESULTS ON TASK 2 BED MATERIAL LEACHATES

	LTL 1 WK			
	6-W380L	10R-W180L	12R-W275L	14-W170L
Aluminum	0.38	0.43	0.39	0.40
Arsenic	<5.0	<5.0	<5.0	<5.0
Boron	<0.5	<0.5	<0.5	<0.5
Cadmium	<0.02	<0.02	<0.02	<0.02
Calcium	950	915	940	940
Chromium	<0.1	<0.1	<0.1	<0.1
Copper	<0.2	<0.2	<0.2	<0.2
Iron	0.46	0.43	0.42	0.45
Lead	<0.5	<0.5	<0.5	<0.5
Magnesium	<0.1	<0.1	<0.1	<0.1
Manganese	<0.02	<0.02	<0.02	<0.02
Molybdenum	<0.1	<0.1	<0.1	<0.1
Nickel	<0.1	<0.1	<0.1	<0.1
Phosphorous	<0.5	<0.5	<0.5	<0.5
Potassium	1.6	1.6	2.3	4.5
Selenium	<5.0	<5.0	<5.0	<5.0
Silicon	0.99	0.94	0.97	1.0
Silver	<0.2	<0.2	<0.2	<0.2
Sodium	3.0	7.6	2.4	8.6
Strontium	17.0	19.0	2.4	2.3
Titanium	<0.2	<0.2	<0.2	<0.2
Zinc	<0.1	<0.1	<0.1	<0.1
Zirconium	<0.1	<0.1	<0.1	<0.1

2.3 Regional Energy Policy Program for the Northern Great Plains

REGIONAL ENERGY POLICY PROGRAM
FOR THE NORTHERN GREAT PLAINS

Quarterly Technical Progress Report for the Period
January - March 1990

by

University of North Dakota
Energy and Environmental Research Center
Box 8213, University Station
Grand Forks, ND 58202

Contracting Officer's Technical Representative: John Byam

for

U.S. Department of Energy
Morgantown Energy Technology Center
P.O. Box 880
3610 Collins Ferry Road
Morgantown, WV 26507-0880

May 15, 1990

Work Performed Under Cooperative Agreement No. DE-FC21-86MC10637

TABLE OF CONTENTS

1.0 INTRODUCTION

The United States is the world's leading consumer of energy. The production and consumption of energy varies over the country as a function of climate, the availability of natural resources, economics, and culture. The northern Great Plains region (Montana, Wyoming, North Dakota, and South Dakota), an area characterized by many similarities in climate, culture, and physiography:

- Accounts for over 10 percent of domestic hydrocarbon production, a major share of low-rank, low-sulfur coal production, a significant steam-generated electrical capability, and a significant portion of domestic uranium production.
- Contains significant oil shale, geothermal, nuclear, and conventional fossil fuel resources.
- Contains significant research capability, particularly with regard to coal-conversion, and oil shale technologies and the environmental effects of fossil fuel production, conversion, and utilization.
- Is a net exporter of energy and fossil fuel materials.
- Is a significant consumer of fuel and fossil fuel by-products in the agricultural sector.
- Receives significant revenues and economic support from fossil fuel exploration, production, conversion, and transportation industries, as well as from ancillary industries.

2.0 PROGRAM OBJECTIVES

Energy-related activities are significant in the economy at the regional, state, and local levels. Fluctuations in energy markets can have marked effects on government revenues and programs as well as on the economy. Since the end of the Second World War, the northern Great Plains has experienced economic "booms" related to oil and gas, coal, oil shale, hydroelectric power, and uranium. Since the early 1970s, the energy market has had to deal with the increase in environmental awareness and the growth and diversification of energy sources and suppliers on a global scale. For example, prospects for the continued growth of the region's coal sector depend to a significant degree on the the nature of federal actions with respect to air quality and waste management. Currently, an attempt is being made during the development of a National Energy Strategy (NES) to take into account the mix of environmental, fiscal, social, research, economic, national security, and resource issues that form the energy picture of the nation. Ensuring the optimal production and utilization of the region's energy resources, within the framework of the developing NES, could be enhanced by responses and initiatives both at the state and regional levels. Once the basic framework of the strategy is in place, periodic review of the policy with respect to the region would be augmented by ready access to pertinent data for the region. To this end, the objectives of the Regional Energy Policy Program for the

northern Great Plains as originally proposed were to:

- Gather, develop, and disseminate information necessary for well-founded energy initiatives in the region.
- Promote and assist in the integration and coordination of the energy-planning efforts of individual states in the region.
- Foster communication between the public and private sector concerning energy-planning needs in the region.
- Achieve objectives and carry out activities in a manner consistent with the National Energy Strategy.

The mission of the Energy Policy Program for the northern Great Plains can best be achieved through an information clearinghouse/data center. We are proceeding in this direction with the development of the "Energy Policy Information Center (EPIC) for the northern Great Plains".

3.0 YEAR 1 GOALS/ACTIVITIES

Year 1 efforts of the Regional Energy Policy Program for the northern Great Plains were designed to initiate the development of an up-to-date listing of energy resources, production, and consumption in the region, as well as a computer-based system to facilitate the efficient identification, collection, and manipulation of energy-related information.

TASK A. Development of an Information Management System

The initial efforts of the program will focus on the identification, acquisition, and organization of pertinent energy information and the development of a computer-based system to manage this information.

TASK B. Compilation of an Annotated Bibliography

The review of information in Task A will form the basis for initiation of an annotated bibliography.

TASK C. Compilation of an Energy Resource Data Base

The review of information acquired in Task A will form the basis for initiation of an energy resource data base.

TASK D. Annual Report

4.0 ACCOMPLISHMENTS

During the first and second quarters (the last half of August 1989 until December 31, 1989) activities included: 1) acquiring computer hardware (a.1), 2) identifying and characterizing pertinent data bases and information sources (a.2), and 3) initiating a literature search (a.3, b.1, b.2). During the third quarter, efforts focused on:

1) The continuation of work on Tasks A & B.

   Task A. Development of an Information Management System

   During this period, the identification and assessment of energy-related data bases for the region (subtask a.2) continued.

   Task B. Completion of an Annotated Bibliography

   During this period, the acquisition and review of relevant documents (subtask b.2), begun in the second quarter, continued. In the second quarter, a preliminary review of computer data bases indicated that over one thousand citations were available for the northern Great Plains. Following a preliminary review over 200 of these references were ordered. In addition, a significant number of references, not listed in the computer data bases, have been noted and are being ordered. Bibliographic information for these documents is being entered in a standardized computer-based Q&A software package format (subtask b.1). Reviews are progressing as time allows.

2) Tracking the developing National Energy Strategy (NES) through discussions with personnel in the Department of Energy Office of Policy, Planning, and Analysis. These activities included: 1) obtaining and reviewing a preliminary draft of the NES, and 2) attendance at a hearing regarding the role of regulation in the energy sector.

3) Initiation of work on Task C: Compilation of an Energy Resource Data Base.

4) Initiation of work on Regional Energy Sector Profiles designed to eventually contain information on occurrence, production, consumption, marketing, environmental issues, regulations, and revenue for each energy source in the region.

5.0 TRIPS/PRESENTATIONS

Trips and presentations during the third quarter included:

Washington, D.C., January 21-24 -- Visited the Office of Policy and Planning, discussions with personnel concerning the status of the NES, obtained and reviewed a draft of the NES and portions of the testimony, and attended a NES hearing on the role of regulation in the energy sector.

6.0 FUTURE ACTIVITIES

Activities in the fourth quarter will include:

1) Continuation of work on Tasks A, B, and C and related activities.

2) Continued tracking of NES developments, including the acquisition and review of the Interim Report on the NES available April 1 as well as the "White Papers" on specific topics which will be available shortly thereafter.

3) Continued contact with energy officials and representatives of the private sector concerning regional policy issues.

4) Initiate the compilation of historical information on federal and regional energy-related initiatives.

3.0 ADVANCED RESEARCH AND TECHNOLOGY DEVELOPMENT

3.1 Turbine Combustion Phenomena

TURBINE COMBUSTION PHENOMENA

Quarterly Technical Progress Report
for the Period January - March 1990

by

Michael L. Swanson, Project Manager
University of North Dakota
Energy and Environmental Research Center
Box 8213, University Station
Grand Forks, ND 58202

Contracting Officer's Technical Representative: Leeland Paulson

for

U.S. Department of Energy
Office of Fossil Energy
Morgantown Energy Technology Center
Morgantown, WV 26507-0880

June 1990

Work Performed Under Cooperative Agreement No. DE-FC21-86MC10637

TABLE OF CONTENTS

LIST OF FIGURES

LIST OF TABLES

TURBINE COMBUSTION PHENOMENA

1.0 INTRODUCTION

Under DOE sponsorship coal/water slurry fuels have been investigated as fuels for gas turbine engines for several years, but the major technical problems still inhibiting commercialization are deposits on the pressure and suction sides of the turbine blades, reducing the gas flow area and the turbine efficiency; acceptable coal burnout, given the short residence time inherent with gas turbine engines; corrosion of turbine blades by condensed alkali sulfates; erosion of turbine blades and other components by ash particles entrained in the products of combustion; and control of NO_x, SO_2, and particulate emissions. The release of certain mineral matter species found in both raw and beneficiated coals can lead to ash deposition on surfaces, regardless of the ash content of the fuel. This deposition can lead to corrosion and metal loss of critical turbine components and, ultimately, to derating, unavailability, or catastrophic failure of the power generation system. Alkali metals and sulfur, existing as impurities in coal, have been identified as key components in the initiation of deposition and the onset of corrosion.

Up to the last four years, low-rank coals (LRCs) were not considered as potential fuels for gas turbine engines because of their high intrinsic moisture levels. It is extremely difficult to prepare a pumpable slurry of as-mined lignite with a dry solids loading over 35 wt.%, due to the high moisture levels in LRCs. However, with the advent of the University of North Dakota's Energy and Environmental Research Center's (UNDEERC's) hydrothermal treatment process, micronized lignite slurries have been produced with a solids loading up to 50% and a heating value over 6000 Btu per pound of slurry. Subbituminous coals also respond very well to hydrothermal treatment and produce higher quality slurries. Availability of a slurry with a high enough fuel value to sustain combustion makes it possible to take advantage of the desirable characteristics of low-rank coals, namely the higher reactivity of its nonvolatile carbonaceous components. Thus a low-rank coal slurry should require less residence time in the gas turbine combustor for complete combustion, or inversely, the coal would not have to be micronized as fine to achieve the same level of burnout, thereby reducing fuel preparation costs. Another potential advantage of low-rank coal slurries is their nonagglomerating tendency relative to bituminous slurries, reducing the importance of atomization to very fine droplet sizes.

2.0 GOALS AND OBJECTIVES

The overall objective of this research is to continue to expand the data base on the effects of low-rank coals' unique properties on its combustion behavior in pressurized combustion systems such as gas turbine engines. Research will be directed toward understanding the properties of LRC fuels which affect ignition and burn times, combustion efficiency, vaporization and deposition of inorganics, and the erosion of critical gas turbine components. Special emphasis will be placed on an investigation of LRC high-shear rheology

and its effect on atomization and combustion behavior, an evaluation of LRCs' nonagglomerating properties using laser-based diffraction techniques (Insitec PCSV), an investigation of particulate hot-gas cleanup techniques, and inorganic transformations/alkali vaporization using a pressurized drop-tube furnace.

2.1 Years Four Through Six Project Objectives

A. Revise Technology and Market Assessment.

This literature review will enable UNDEERC personnel to assess the current status of coal-fired gas turbine research to determine what recent advances have been made by other researchers. This effort will build upon the technology and market assessment made at the start of this program.

B. Characterization of LRCs' Atomization Properties.

The objective of this task is to investigate the effects of coal type, particle-size distribution, solids loading, additive package, and shear rate on LRC slurry rheology. High-shear rheology will be measured using a capillary extrusion viscometer modified to perform rheological tests at shear rates up to 200,000 1/sec. This task will also examine the pressurized atomization characteristics of these LRC fuels with a Malvern 2600 particle-size analyzer and still photography in a pressurized spray chamber under construction at UNDEERC. The combustion behavior of these same fuels will be evaluated under similar air-to-fuel and pressure ratios in the gas turbine simulator. This task would also look at different atomizer types in a effort to minimize spray droplet size distributions for a given rheology and atomizing air-to-fuel ratio.

C. Evaluation of LRC Fuel Agglomeration.

The objective of this task is to evaluate the agglomerating or nonagglomerating tendencies of LRC fuels by providing optical access for an Insitec PCSV particle-size analyzer at various residence times along the axis of a pressurized drop-tube furnace under construction at UNDEERC. Thus product of combustion (POC) particle-size distributions as a function of residence time, the starting particle-size distribution, and droplet size can be measured to determine if the smaller particle-size distributions found in the LRC fly ash are the result of a gradual burnout of slurry droplet agglomerates or the result of agglomerate disintegration into its original particle-size distribution due to the high thermal friability of LRC fuels.

D. Investigation of Particulate Hot-Gas Cleanup Systems.

The objective of this task is to evaluate potential hot-gas particulate cleanup techniques as to their relative probability of success and to test the best two or three systems in the turbine simulator. This task would include a technology assessment building upon a previous literature search performed on hot-gas cleanup techniques. These techniques

could include, but would not be limited to, ceramic cross flow filters and filter candles, nested fiber filters, cyclones, HTHP ESPs. Potential also exists for investigating an alkali vapor cleanup device (i.e., sorbent-packed beds, etc.).

E. Ash Transformation and Alkali Vaporization Studies.

The objective of this task is to investigate the ash transformations experienced by the mineral matter in beneficiated low-rank coal fuels. Very little research to date has investigated the effects of pressure and coal beneficiation on the reaction pathways taken by the mineral matter present in LRC fuels. These transformations should be dependent on the cleaning techniques used and the level of cleaning achievable on the various coal types. Mineral matter transformations of beneficiated LRC under turbine operating conditions will be investigated in a pressurized drop-tube furnace under construction at UNDEERC. This drop-tube furnace will be capable of combusting both slurry droplets and coal particles. The effects of residence time, temperature, pressure, atmosphere, and gas/fuel flow rates can be varied to examine their effects on ash transformations and carbon burnout. The drop tube will also provide carbon burnout as a true function of residence time, given the laminar gas flow. The effects of deposition probe shape and temperature and approaching gas velocity on the measured deposition rates can also be investigated. Optical ports into the drop tube will enable quantities of alkali vapor/aerosols in the gas streams to be measured using in situ methods. Another advantage of the pressurized drop-tube furnace is the small quantities of fuel (up to 1.5 lbs/hr) needed to conduct extensive deposition and burnout testing as compared to the turbine simulator (approximately 150 lbs/hr).

F. Investigation of Slagging Combustor Design.

Should concurrent beneficiation of LRC studies at UNDEERC indicate that acceptable ash levels and composition not be achievable, a vertically fired combustion zone would be built to replace the horizontally fired rich combustion zone on the current turbine simulator. This modification would enable the combustor to operate in a slagging combustor mode versus the current nonslagging combustor mode. Work on this task would be dependent on the results of the work in progress and would be subject to DOE approval.

2.2 Fourth Year Goals and Objectives

Task A - Revise Technology and Market Assessment.

This task involves updating the previous literature assessment made at the beginning of the program.

Task B - Characterization of LRCs' Atomization Properties.

This task involves the investigation of LRCs' fuel atomization and viscosity properties using a capillary viscometer and a pressurized spray

chamber with a Malvern particle-size analyzer and still photography to determine spray droplet sizes. In addition, this task will conduct a parametric investigation of different atomizers for atomization effectiveness. This includes the commercially available Delavan and Parker-Hannifan atomizers, along with the UNDEERC developed B-II nozzle. This task will also evaluate atomizer combustion performance under the same operating conditions in the turbine simulator combustion rig.

Task C - Evaluation of LRC Fuel Agglomeration

This task consists of using laser-based diagnostics (i.e., Insitec PCSV) and particulate sampling to determine if LRC slurry droplets are friable enough to break into their original particle sizes as hypothesized or remain as agglomerates which must burnt out.

Task D - Investigation of Particulate Hot-Gas Cleanup Systems.

This task involves evaluating potential hot-gas particulate cleanup techniques for use in direct coal-fired gas turbines to test the two best techniques in combustion tests on the turbine simulator. These techniques could include, but would not be limited to, ceramic cross flow filters and filter candles, nested fiber filters, cyclones, HTHP ESPs, etc.

Task E - Ash Transformation and Alkali Vaporization Studies.

Technical work in this task for Year 4 consists of finishing construction on the PDTF and subsequent combustion tests using selected beneficiated coals to determine the effects of residence time, gas composition, temperature, and pressure on carbon burnout and ash deposition.

Task F - Investigation of Slagging Combustor Design.

No technical work in this task will be performed in Year 4. If coal ash properties dictate, construction of a first-stage slagging combustor would begin late in Year 5.

3.0 BACKGROUND

3.1 One Million-Btu/hr Gas Turbine Combustor

To meet the objectives of the program, a pressurized combustion vessel was built to allow the operating parameters of a direct-fired gas turbine combustor to be simulated. One goal in building this equipment was to design the gas turbine simulator as small as possible to reduce both the quantity of test fuel needed and the test fuel preparation costs, while not undersizing the combustor such that wall effects would have a significant effect on the measured combustion performance. Based on computer modeling, a rich-lean, two-stage nonslagging combustor has been constructed to simulate a direct-fired gas turbine. This design was selected to maximize the information that could be obtained on the impact of the unique properties of low-rank fuels and

various hot-gas cleanup techniques on the gas turbine combustor and its turbomachinery.

A short description of the gas turbine simulator is given here; a more detailed description is given elsewhere (1,2,3). Figure 1 is a schematic of the 1-MM Btu/hr gas turbine combustor, showing its internal design. Figure 2 is a photograph of the 1-MM Btu/hr gas turbine combustor. The head section of the turbine has an interchangeable, horizontal, flat-bladed air swirler for controlling the primary air-fuel spray and developing a recirculation zone in the rich combustion zone. A Delavan Swirl-Air nozzle with a 50° spray angle is currently used as the atomizer. The pressurized combustion vessel itself is comprised of several short sections of refractory-lined stainless steel pipe. These sections are water-jacketed to provide cooling of the external pressure vessel wall. This modular design allows the length of the combustion zones to be varied. The removal of some of these modules allows the effect of residence time to be investigated under similar flow conditions.

The quench zone of the turbine simulator was designed to promote rapid mixing of the secondary air with the POC exiting the rich combustion zone, thus minimizing the occurrence of localized "hot spots" and the formation of thermal NO_x. A rotary control valve and a high-temperature guided seat control valve are used to control the flow of combustion air entering the air preheater and the distribution of air between the rich and lean zones, respectively. The combustor is designed to operate at pressures up to 250 psig and a lean zone exit temperature of 2000°F.

A reduced flow area in the deposition section is used to increase the gas velocities up to those typically seen in the expander section of a gas turbine (400 to 800 ft/sec). Four air-cooled probes with various contact angles were machined from thick-walled high-temperature alloy tubing and were installed to simulate the leading edge of turbine blades. Additional cooling air was added after the first two probes to cool the exit gas stream up to 200°F, such that gas temperature as well as metal temperature can be investigated for their effects on deposition/erosion/corrosion (DEC). A spray water quench zone is located after the deposition section to spray high-pressure water into the combustion gases to cool the gases before passing them through the rotary control valve used to back pressure the turbine simulator. A natural gas-fired fluidized bed preheater is used to preheat the high pressure combustion air to temperatures as high as 1000°F. Combustion efficiencies of the test fuels fired in the turbine simulator are calculated from gas and isokinetic particulate samples taken from both the rich and lean zones of the combustor.

3.2 Scanning Electron Microscope Techniques

Computer-controlled scanning electron microscopy (CCSEM) is used to characterize minerals in unaltered coal samples and inorganic phases in combustion products such as char or fly ash. A computer program is used to locate, size, and analyze particles. Because the analysis is automated, a large number of particles can be analyzed quickly and consistently. The heart of the CCSEM analysis system is a recently installed annular backscattered electron detector (BES). The BES system is used because the coefficient of

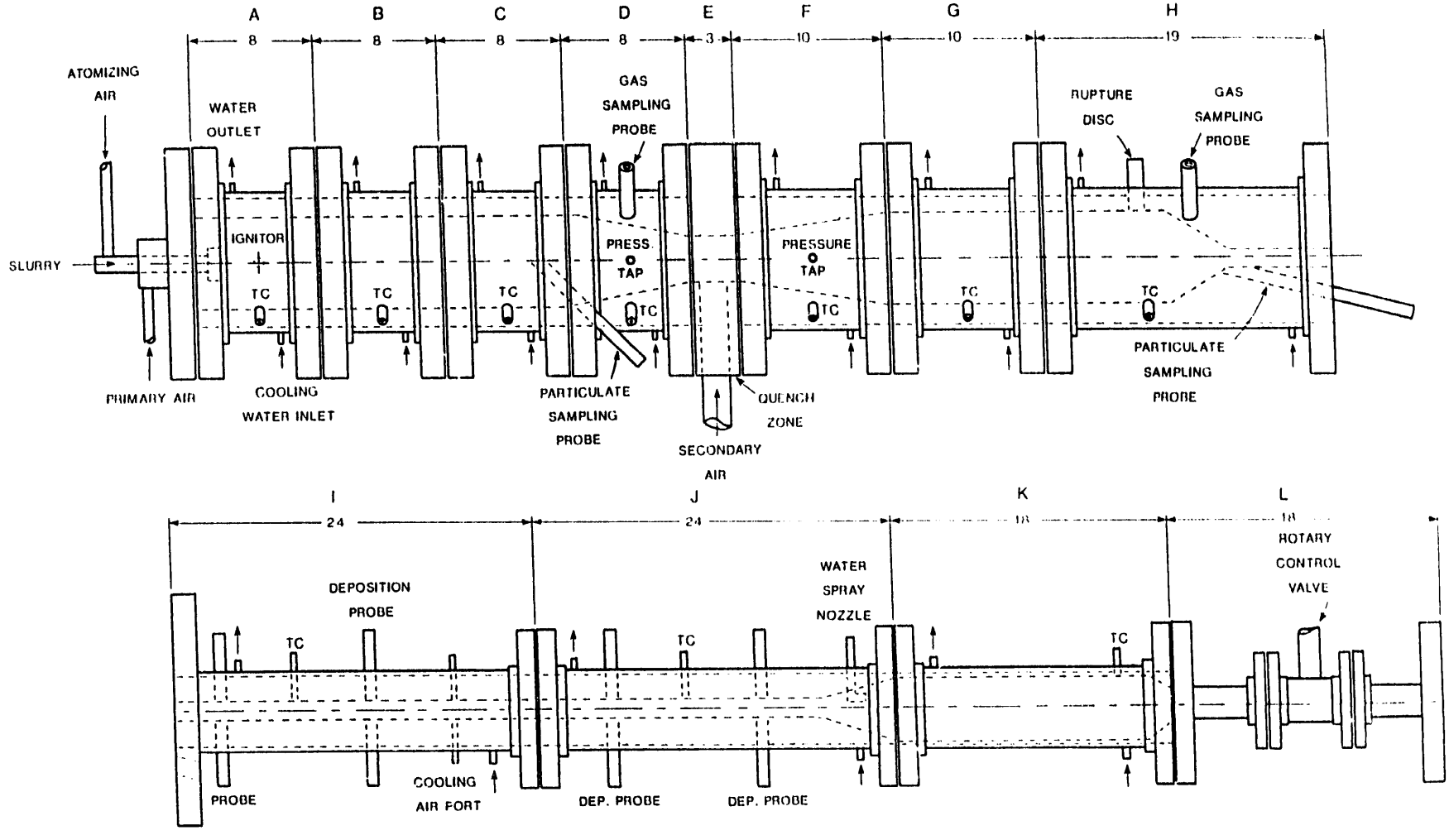

Figure 1. Schematic of 1-MM Btu/hr gas turbine simulator.

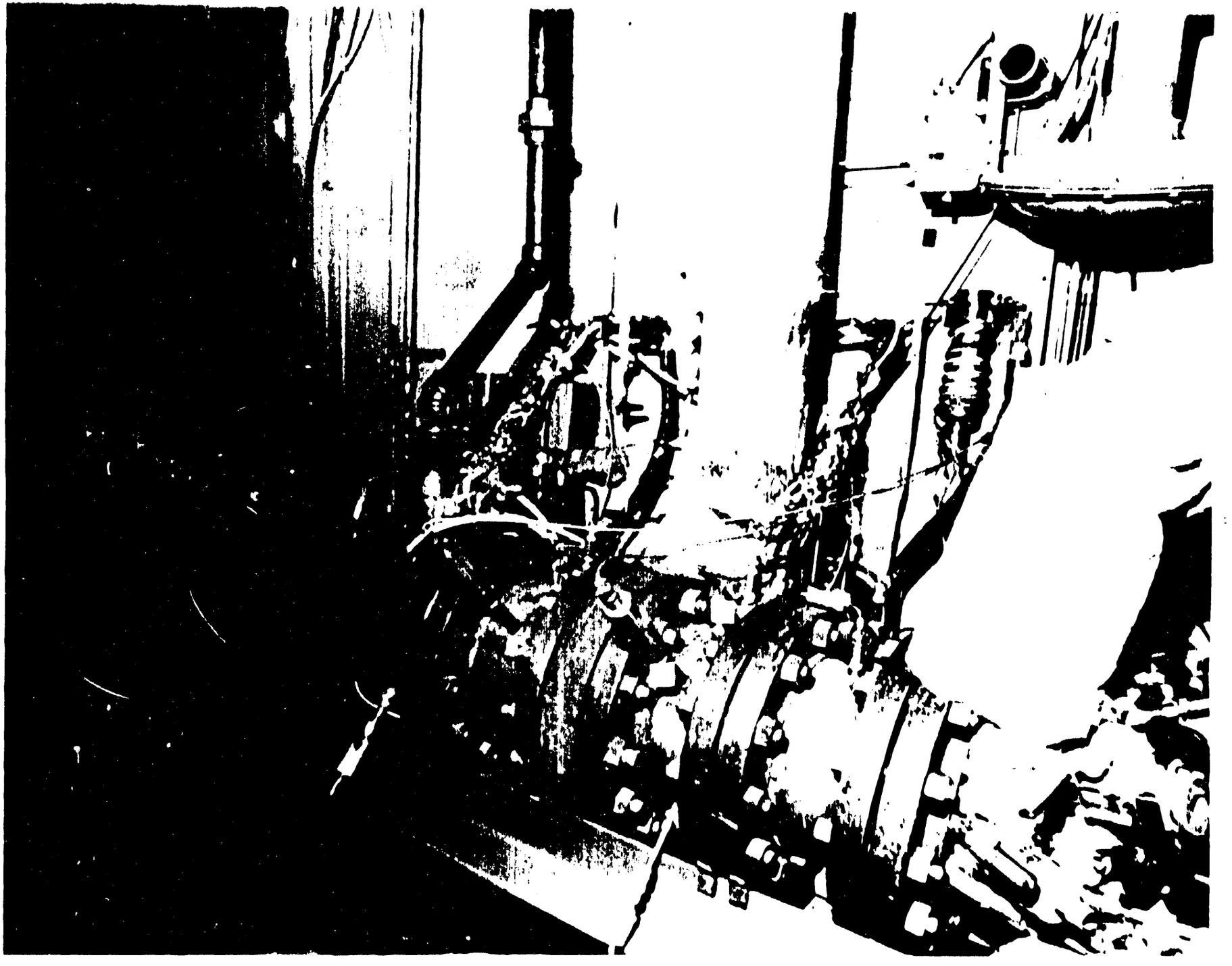

Figure 2. Photograph of 1-MM Btu/hr gas turbine simulator.

backscatter (the fraction of the incoming beam that is backscattered) is proportional to the square root of the atomic number of the scattering atoms. This permits a high degree of resolution between sample components based on their atomic numbers. This means that coal minerals can be easily discerned from the coal matrix, and fly ash particles can be easily discerned from epoxy in polished sections. Brightness and contrast controls are used to optimize threshold levels between the coal matrix and the mineral grains or fly ash particles. When a video signal falls between these threshold values, a particle is discerned, and the particle center is located. A set of eight rotated diameters about the center of the particle are measured, and the particle area, perimeter, and shape are calculated. The beam is then repositioned to the center of the particle, and an x-ray spectrum is obtained. The information is then stored to a Lotus™ transportable file for data reduction and manipulation. The CCSEM data provides quantitative information concerning not only the mineral types which are present, but their size and shape characteristics as well. Since the same analysis can be performed on the initial coal and resultant fly ash or char, direct comparisons can be made and inorganic transformations inferred.

In order to quantitatively determine the distribution of phases in fly ashes, deposits, and slags, the scanning electron microscopy point count technique (SEMPC) was developed. The method involves microprobe analysis of a large number of random points in a polished cross section of a sample. The quantitative analysis of each point is transferred for data base analysis. The software is used to calculate molar and weight ratios for each point. Using these ratios, the points which have compositions of known phases (common to ashes and coal minerals) are identified and counted. The software then finds the relative percents of all the identified points as well as the percent number of unknown phases. The unknown phases are those for which there is no known phase corresponding to the chemical composition. In addition, the average chemical composition of all the points in the sample is calculated. Previous work at UNDEERC has shown that the SEMPC average composition corresponds very well to the bulk chemical analysis (4). The quantitative ability of the SEMPC allows for detailed comparisons to be made between different samples.

4.0 ACCOMPLISHMENTS

4.1 Detailed Design of a High-Temperature, High-Pressure Cyclone

A high-temperature, high-pressure (HTHP) cyclone was selected as the first stage in a particulate hot-gas cleanup device. The design goal was to remove 95% of 5-micron particulate. The cyclone was also designed to fit inline with the current turbine simulator located at the UNDEERC. Design conditions were selected to match those experienced in the turbine simulator at its 1-MM Btu/hr firing rate. These conditions resulted in a gas flow rate of approximately 400 scfm entering the cyclone at 2000°F and 160 psig. Cyclone dimensions were selected using the dimensions reported by Perry (5) and Stairmand (6). Table 1 shows the calculated collection efficiency and pressure drop of the HTHP cyclone at different diameters. Using the methodology reported by Lapple (7), a cyclone diameter of 5 inches was calculated to

TABLE 1

HIGH-PRESSURE, HIGH-TEMPERATURE CYCLONE DESIGN RESULTS AT 400 SCFM, 175 PSIA, AND 2000°F

Cyclone Diameter (in.)	50% Cut Size (μm)	Collection Efficiency (@ 5 μm)	Differential Pressure (in H_2O)
5.5	2.51	0.80	46.7
5.0	2.17	0.84	68.3
4.5	1.86	0.88	104.1
4.0	1.56	0.91	166.8
3.5	1.27	0.94	284.5

provide a collection efficiency of approximately 85% for 5-micron particles and to have a pressure drop less than 2.5 psi.

Figure 3 is a drawing showing the design of the high-temperature, high-pressure (HTHP) cyclone which will be inserted in the turbine simulator combustion system located at the UNDEERC. This cyclone will be fabricated from 8-inch schedule 40 pipe which is welded to form an off-center tee. This pipe will be water-jacketed to keep the metal wall temperatures low. As shown in Figure 3, the cyclone dimensions will be cast in refractory inside the tee. This cyclone will replace the last section of the lean combustion zone shown in Figure 1. Openings have been included in the vessel walls for measuring the inlet and outlet combustion gas temperatures and pressures. In addition, openings have also been included for taking upstream particulate samples, while an existing port will allow downstream particulate samples to be collected for measuring the cyclone efficiency. A second opening was added for a water-jacketed and sealed boroscope viewing system which is currently being ordered. This boroscope will allow the flame quality and stability to be monitored during combustion tests.

4.2 Pressurized Spray Chamber

Due to emphasis on completing the pressurized drop-tube furnace and a busy construction schedule for the operations group with large pilot plant-scale projects in circulating fluid-bed combustion and mild gasification, atomization testing has been postponed until more operator time becomes available.

4.3 Design and Construction of a Pressurized Drop-Tube Furnace

The emergence of advanced coal combustion technologies such as coal slurry-fired gas turbines requires fundamental knowledge of the fuel combustion processes at elevated pressures. Of critical importance is the basic combustion kinetics and the fate of coal mineral matter in such systems. To address these issues, a pressurized drop-tube furnace is being constructed.

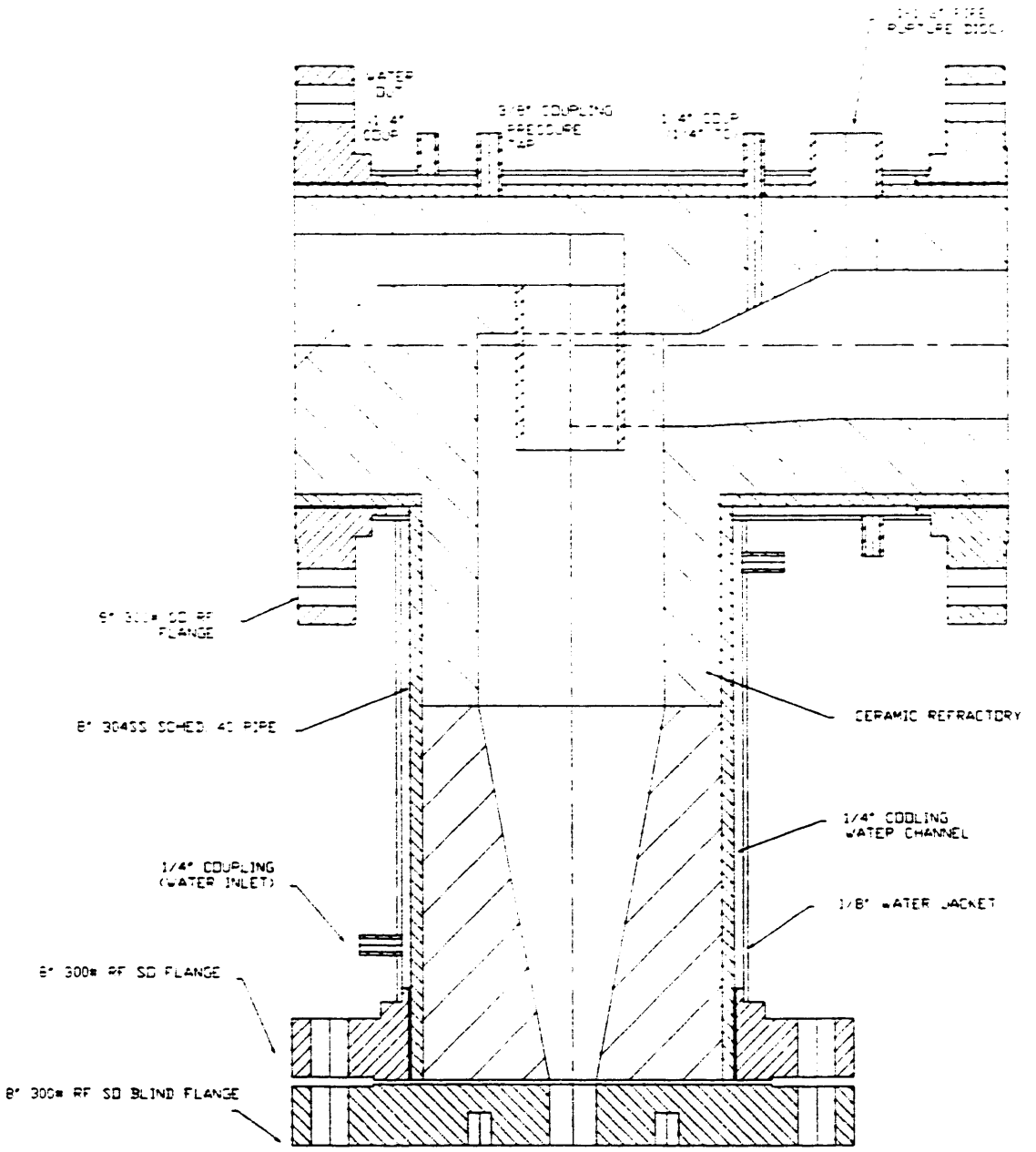

Figure 3. Design of HTHP cyclone for testing in 1-MM Btu/hr gas turbine simulator.

The pressurized drop-tube furnace (PDTF) is capable of operating under the following conditions:

Temperature: ambient to 1500°C
Pressure: ambient to 20 atm.
Oxygen: 0 - 20 mole%
Gas Flow: 0 to 400 slpm at 20 atm.
Residence Time: 0 to 0.50 sec.

- Optical access at any residence time
- Provision for char and ash collection
- Provision for ash deposition studies

The design of the PDTF incorporates several novel features which will allow the design goals to be met. A drawing of the PDTF facility is given in Figure 4. The entire PDTF is constructed of standard 24" and 6" flanged pipe sections. The large pressure vessel contains the furnace sections of the PDTF as shown in Figure 5. Figure 6 is a photograph of the PDTF after assembly for shakedown testing. The walls of the vessel are water-cooled to dissipate the heat from the furnaces. There is a preheater and two furnace sections located above the optical sight ports and one furnace below the optical sight ports to reduce the temperature gradient across the optical access section. Optical access is provided by four 3" diameter ports in the pressure vessel. Electrical power is supplied to the furnaces by electrical feedthrough terminals in the bottom blind flange of the pressure vessel.

Above the large pressure vessel shown is the injector section containing the injector assembly. The injector is a one-inch diameter water-cooled probe sheathed in high-temperature insulation. Figure 7 is a photograph showing the translating mechanism used for raising and lowering the injector into the ceramic tube inside the furnace assembly. The injector may be retracted completely out of the furnace when not in use or may be lowered into the furnace to give the desired residence time between zero and 0.5 seconds. Small viewports in the pipe crosses at the bottom and top of the injector section allow visual inspection of the probe and the sample-feeding behavior.

Below the large pressure vessel is a similar collection assembly and translation mechanism. The collector may be raised to the level of the optical access ports and retracted completely from the furnace for the removal of sample deposits or when not in use. Two pipe crosses with small sight ports allow inspection of the collection probe operation, and the removal of a blind flange provides access for the removal of sample deposits. Both assemblies are interchangeable to allow for feeding powdered or slurry fuels and for collecting deposition or fly ash samples.

The sample feeder assembly is a blank flanged 6" pipe cross pressurized to slightly above the furnace pressure with gas connections to the furnace assembly. Figure 7 also shows the sample feeder pressure vessel located next to the sample injector translating mechanism. The design allows the actual sample feeder to be constructed of lightweight material, since it does not have to withstand more than slight pressure differentials. A small sight port allows inspection of the feeder operation, and the removal of a blind flange gives access to the vessel for filling or adjustment of the feeder. The lightweight feeder can then hang from a load cell in the pressure vessel to provide a continuous record of the sample feed rates. The gas composition and flow rate of gas into the PDTF is controlled by oxygen and nitrogen mass flow controllers. Gas composition can be controlled between 0-20 mole% at flow rates up to 400 liters/minute. The furnace pressure is controlled by a letdown control valve at the exit of the furnace.

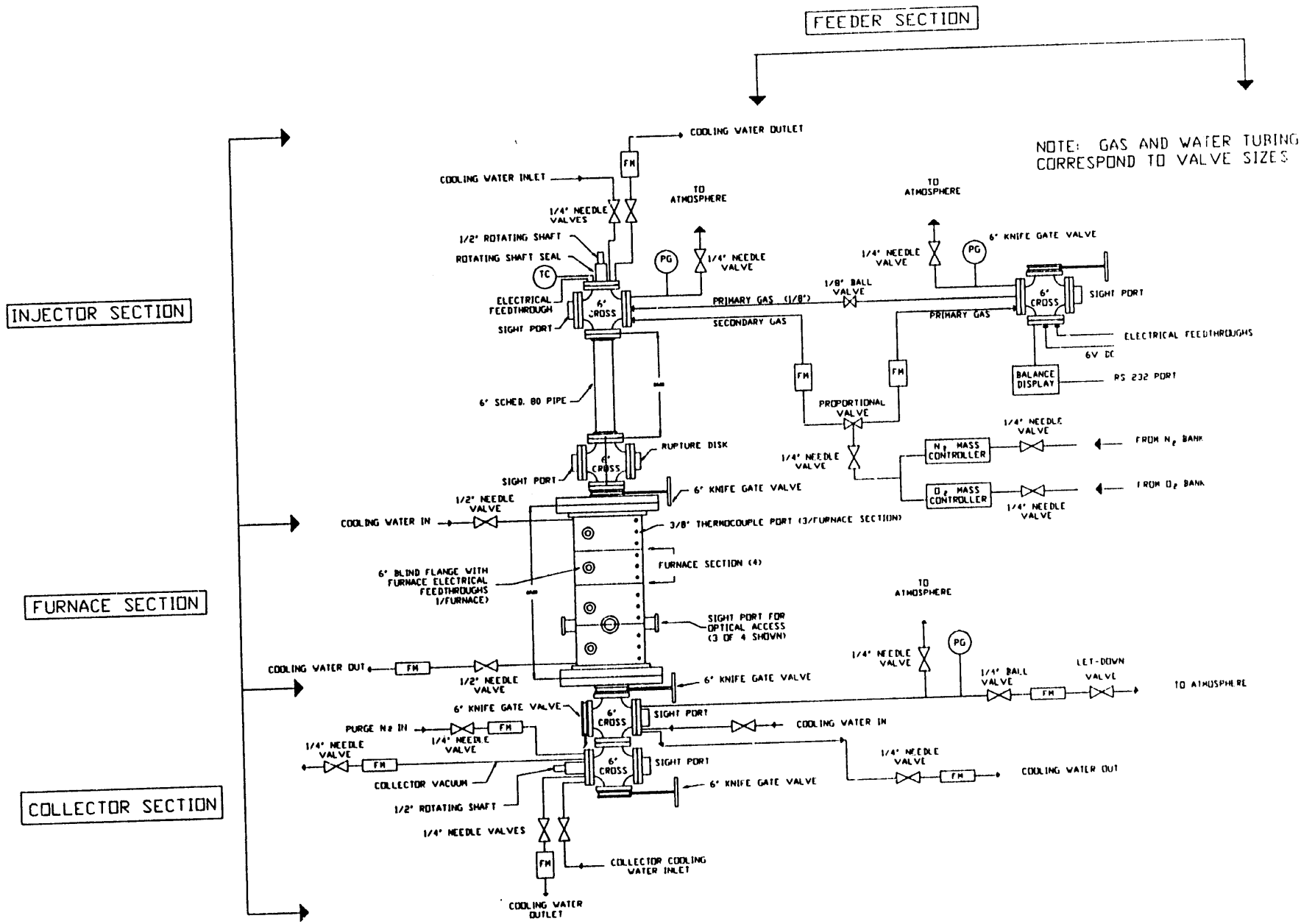

Figure 4. Pressurized drop-tube furnace process schematic.

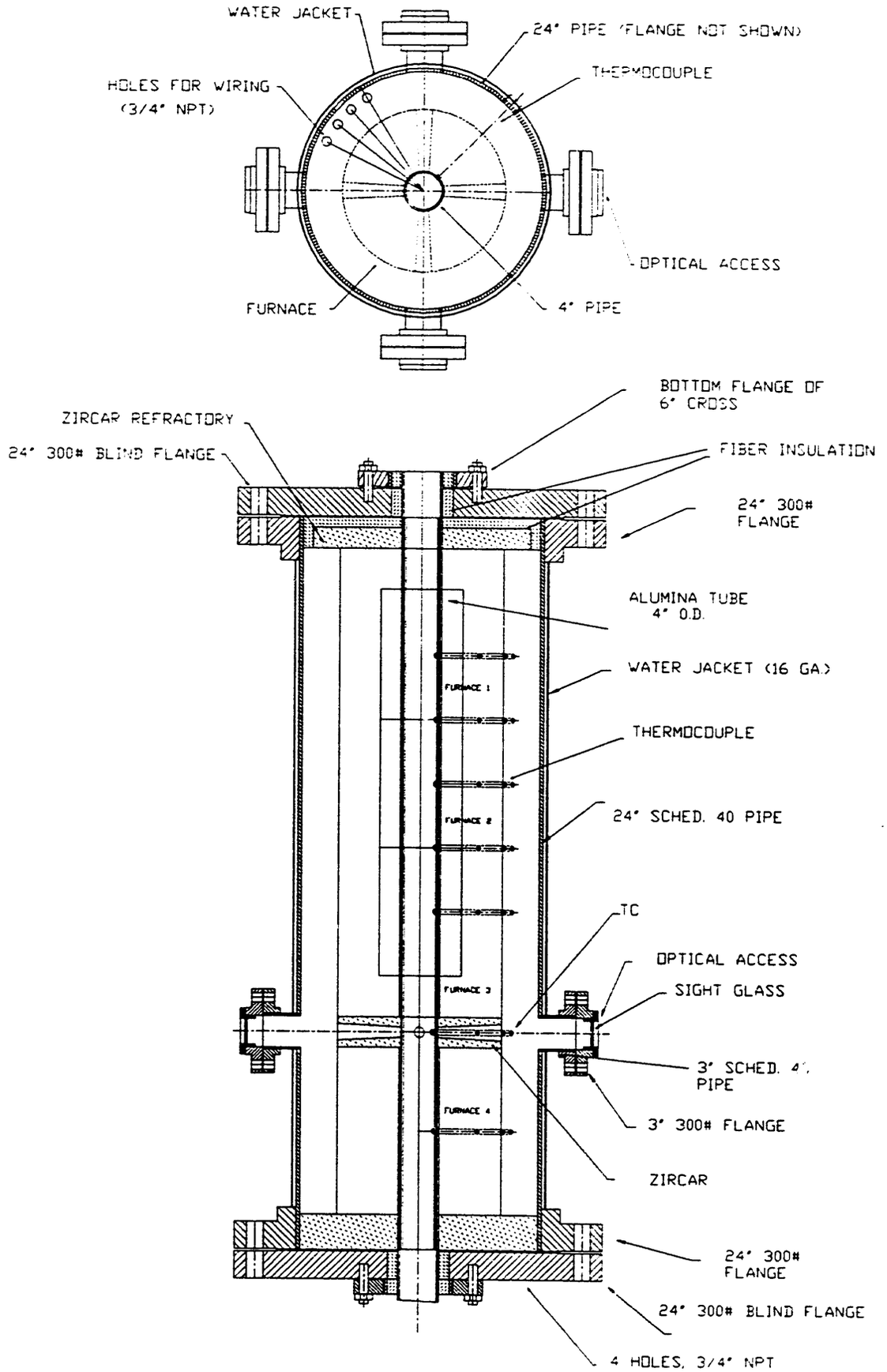

Figure 5. Furnace assembly in PDTF vessel.

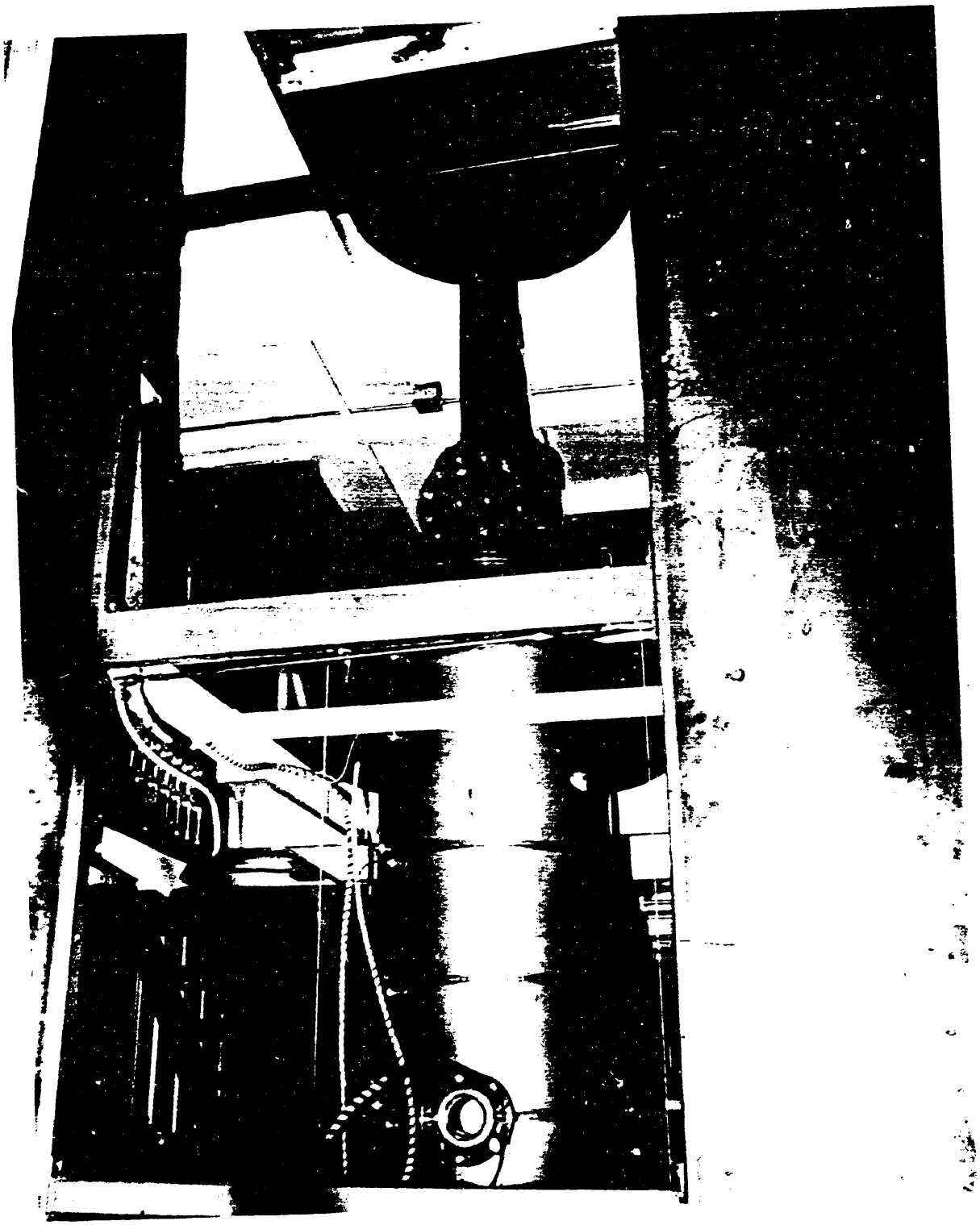

Figure 6. Photograph of PDTF pressure vessel.

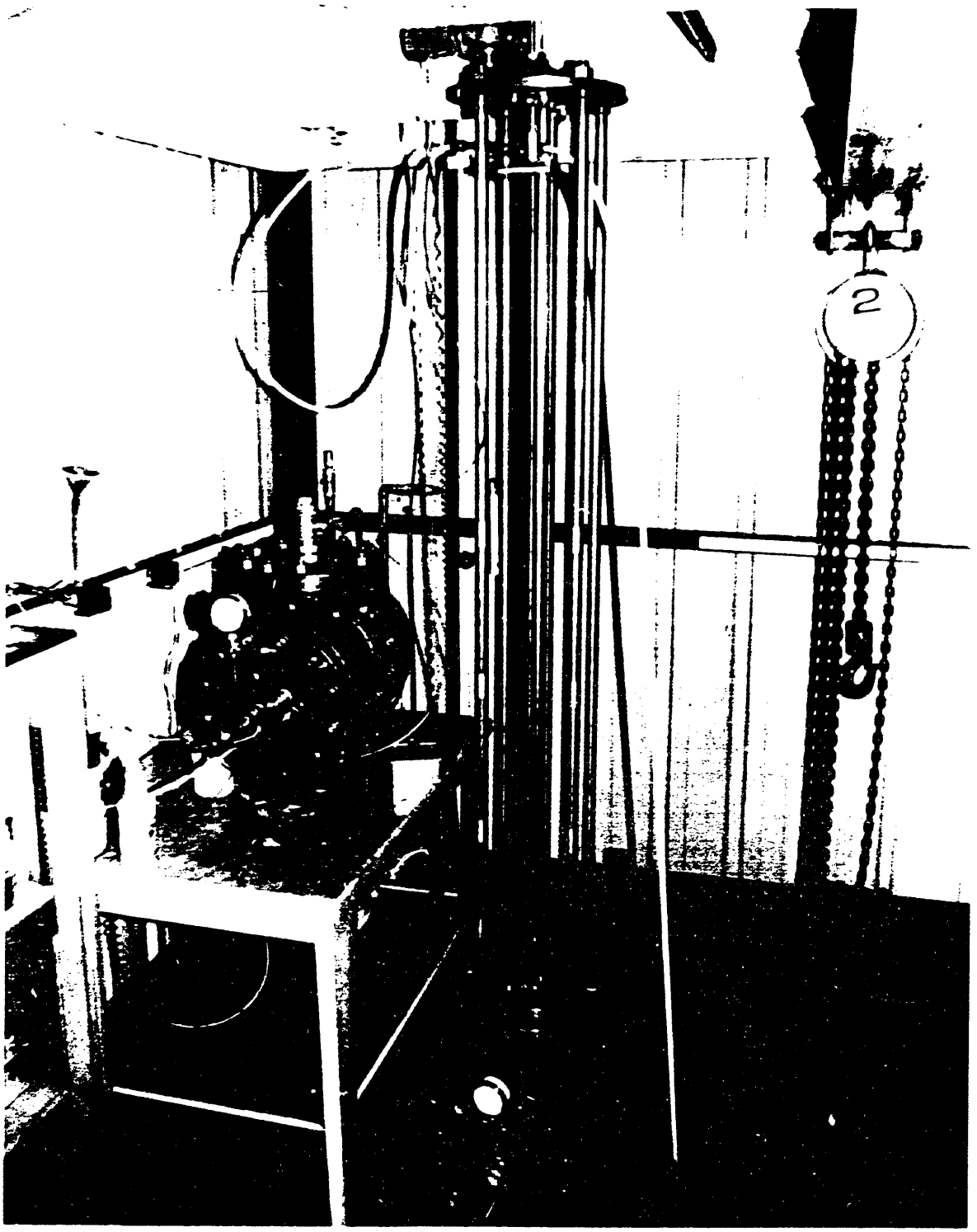

Figure 7. Photograph of PDTF translating mechanisms.

This quarter the furnace sections were mounted and wired in the 24-inch pressure vessel, and the optical insulation and all other insulation were installed. All the pressure vessel sections were reassembled and torqued to their proper setting. All thermocouple, pressure transducer, and mass flow controller wiring was completed. The water-cooled injection and sampling probes were fabricated, and the portions which would be inserted in the hot furnace were covered with insulation. These probes and their translating mechanisms were installed on the PDTF. The translating mechanisms were tested and calibrated to determine the actual location of the probes in the furnace at any given position of the translating mechanism. All cooling water, nitrogen, oxygen, and air lines were plumbed in to the appropriate ports and flowmeters. A coal feeder was fabricated and installed in the separate six-inch cross. Figure 8 is a schematic of the coal feeder used in the PDTF.

The complete system was given a final pressure check at 250 psig. The furnace elements were baked out at 1200°C, according to insulation bakeout procedures. The PDTF furnaces and controllers functioned properly, and the cooling water was found to keep the external air gap around the furnace and the injection and deposition probes at reasonable temperatures. A shakedown test was performed to test the complete PDTF system. During this shakedown testing, several problems were encountered. One problem was that the load cell for monitoring the coal feed rate was too small; thus, the coal feeder used most of the load cell range before any coal was loaded into the feeder. In addition, problems were encountered when feeding coal, due to the PDTF gas flowmeters being sized too small, thus limiting the gas velocity used to pneumatically convey the coal particles into the PDTF. Further examination indicated that the coal was plugging close to the tip of the injection probe. It was also observed that the deposition substrate temperature was too low, due to the substrate being mounted right on the end of the water-cooled deposition probe. A thermal barrier, such as ceramic insulation, will have to be inserted between the probe and the substrate in order to achieve higher metal temperatures. During this testing, the heating elements for the bottom furnace burned out, leading to extremely low gas temperatures being measured in the optical access area. The PDTF will have to be partially disassembled and the furnace repaired before any meaningful testing can be accomplished.

4.4 SEM Analytical Results

CCSEM analyses were performed on the original CWF tested in the 1-MM Btu/hr gas turbine simulator in order to establish a baseline for comparison with deposits generated at 1100°C from these fuels in the PDTF facility. The Otisca CWF is a Taggart seam, Virginia bituminous coal bought commercially from Otisca, Ind. (Syracuse, NY). The Kemmerer and Beulah-Zap fuels were prepared at UNDEERC. The Kemmerer fuel was acid-cleaned only, while the Beulah-Zap fuel was both physically and chemically cleaned, and both were then hydrothermally treated and micronized. Tables 2 and 3 show the proximate and ultimate analyses, ash fusion temperatures, particle-size and x-ray fluorescence analyses previously reported on these fuels.

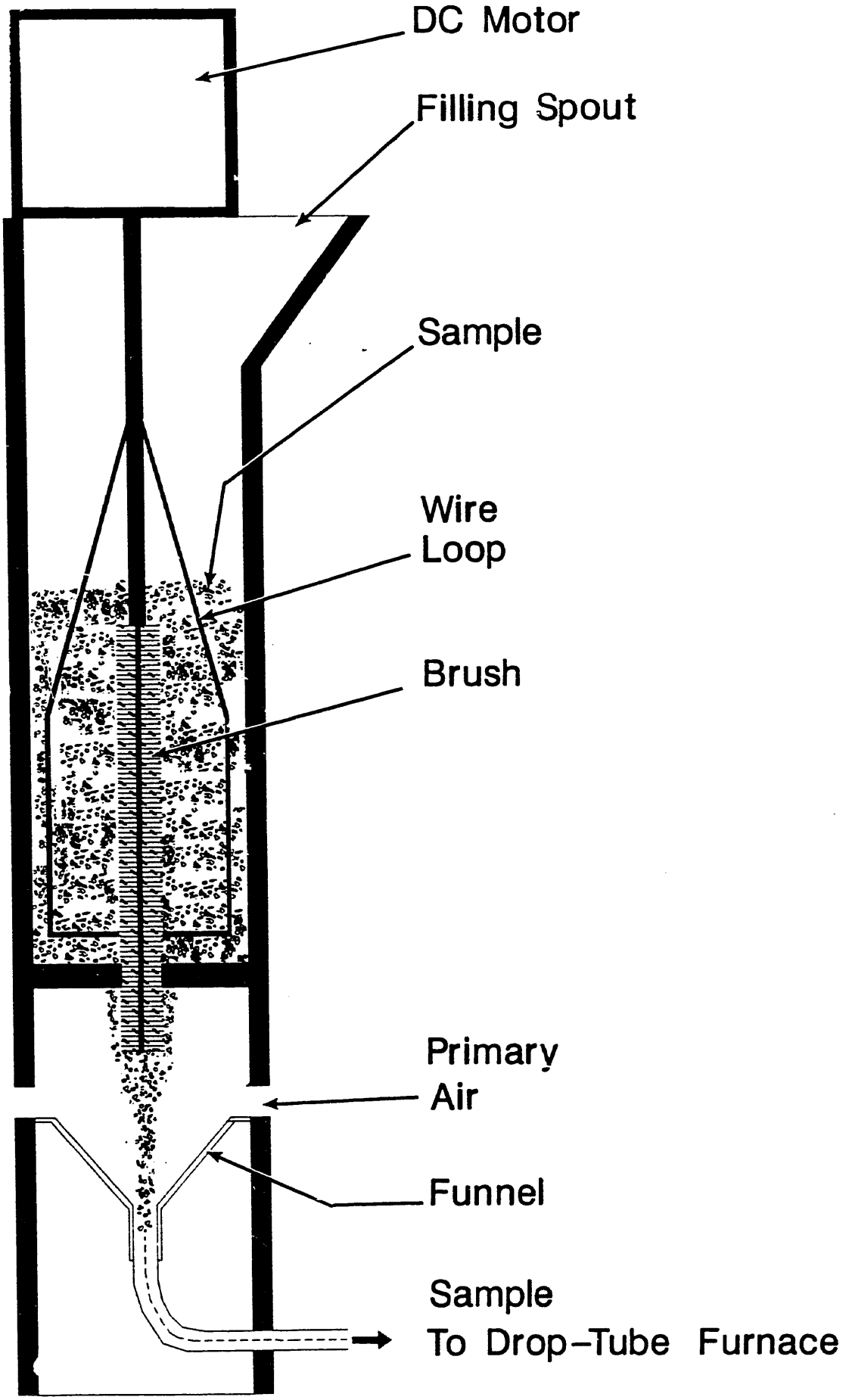

Figure 8. Schematic of coal feeder for pressurized drop-tube furnace.

TABLE 2

PROXIMATE AND ULTIMATE ANALYSES OF LRC FUELS TESTED IN TURBINE PROGRAM

Sample:	Otisca	Kemmerer	Beulah-Zap
PDU Test No.	N/A	38	40
Prox. Analysis (MF)			
Vol. Matter	36.10	41.10	42.66
Fixed Carbon	63.07	56.62	54.78
Ash	0.83	2.28	2.56
Ult. Analysis (MF)			
Hydrogen	5.39	5.03	4.29
Carbon	82.90	75.72	70.89
Nitrogen	1.59	1.30	1.20
Sulfur	0.78	0.26	0.78
Oxygen (by diff.)	8.49	15.40	20.26
Ash	0.83	2.28	2.56
Heating Value (MF, Btu/lb)	15,060	12,925	12,014
Ash Fusion Temperatures (°F-Reducing Atm)			
Init. Deform. Temp.	2119	2000	1942
Softening Temp.	2187	2095	1986
Hemisph. Temp.	2362	2140	2068
Fluid Temp.	2370	2201	2329
Part. Size-Mean (microns)	4.6	10.1	15.9
Top Size (99%<) (microns)	15.2	34.9	59.6

TABLE 3

X-RAY FLUORESCENCE ANALYSIS OF LRC FUELS TESTED IN TURBINE PROGRAM

High-Temperature Ash Results (% of ash, SO_3-free)	Otisca Fuel	Kemmerer Fuel	Beulah-Zap Fuel
SiO_2	37.0	49.0	25.2
Al_2O_3	28.8	22.0	20.5
Fe_2O_3	20.1	14.5	29.2
TiO_2	4.4	1.2	1.8
P_2O_5	0.4	0.4	1.5
CaO	5.7	9.1	16.3
MgO	1.6	3.5	4.8
Na_2O	0.0	0.0	0.0
K_2O	1.8	0.2	0.7

Tables 4, 5, and 6 show the CCSEM analysis performed on these same fuels. The first seven columns are all in weight percent on a mineral basis in a certain size distribution, while the last column is the total weight percent on a coal basis, regardless of size. The analysis for the Otisca CWF shows that there were no minerals above 10 microns and only 16 wt.% of mineral particles were over 4.6 microns. In addition, two compounds (aluminosilicate and pyrite) comprise 60 wt.% of the minerals. The identified mineral phases account for approximately half of the ash level reported in the proximate analysis. For the Kemmerer CWF, quartz, aluminosilicate, and pyrite are the major mineral types. About 38 wt.% of all the minerals are greater than 10 microns. It is interesting to note that quartz comprises approximately 57.5 wt.% of the minerals, and aluminosilicate constitutes another 24 wt.% of the minerals. Approximately 83 wt.% of the ash in the coal is in the mineral form, which is consistent with this fuel being acid-cleaned only.

The major minerals identified in the Beulah CWF are quartz and pyrite; however, the iron oxide level is higher than would be expected for the Beulah fuel and is probably the result of some of the magnetite used in the heavy media separation remaining with the fuel. Approximately 43 wt.% of the minerals in the Beulah fuel are greater than 10 microns. The high level of unknowns is also unusual and merits further examination. Only 9 wt.% of the ash in the Beulah fuel was identified as minerals in the CCSEM analysis. From

TABLE 4

SUMMARY OF CCSEM RESULTS FOR OTISCA FUEL

	Weight Percent Mineral Basis Particle-Size Distribution (μm)							Total wt.%
	<2.2	2.2-4.6	4.6-10	10-22	22-46	>46	Total	Coal Basis
QUARTZ	3.5	3.1	1.0	0.0	0.0	0.0	7.6	0.03
IRON OXIDE	0.7	1.1	2.6	0.0	0.0	0.0	4.4	0.02
ALUMINOSILICATE	14.6	15.7	7.0	0.0	0.0	0.0	37.3	0.16
CA AL-SILICATE	0.1	0.0	0.0	0.0	0.0	0.0	0.1	0.00
FE AL-SILICATE	3.8	1.6	0.0	0.0	0.0	0.0	5.3	0.02
K AL-SILICATE	3.2	4.3	4.4	0.0	0.0	0.0	11.9	0.05
PYRITE	16.4	5.1	1.0	0.0	0.0	0.0	22.5	0.10
GYPSUM	0.8	1.7	0.0	0.0	0.0	0.0	2.4	0.01
BARITE	0.1	0.0	0.0	0.0	0.0	0.0	0.1	0.00
CA SILICATE	0.0	0.2	0.0	0.0	0.0	0.0	0.2	0.00
GYP/AL SILICATE	0.1	0.0	0.0	0.0	0.0	0.0	0.1	0.00
ALUMINA	0.1	0.4	0.0	0.0	0.0	0.0	0.5	0.00
CALCITE	0.0	0.4	0.0	0.0	0.0	0.0	0.4	0.00
RUTILE	0.5	0.3	0.0	0.0	0.0	0.0	0.8	0.00
PYRRHOTITE/SULFA	1.0	0.0	0.0	0.0	0.0	0.0	1.0	0.00
SI-RICH	0.5	0.4	0.0	0.0	0.0	0.0	0.9	0.00
UNKNOWN	3.2	1.4	0.0	0.0	0.0	0.0	4.6	0.02
TOTAL	48.5	35.5	16.0	0.0	0.0	0.0	100.0	0.43

TABLE 5

SUMMARY OF CCSEM RESULTS FOR MICRONIZED KEMMERER

	Weight Percent Mineral Basis Particle-Size Distribution (μm)							Total wt.%
	<2.2	2.2-4.6	4.6-10	10-22	22-46	>46	Total	Coal Basis
QUARTZ	7.5	8.8	8.6	13.3	19.4	0.0	57.7	1.09
IRON OXIDE	0.8	0.6	1.0	0.0	0.0	0.0	2.4	0.05
ALUMINOSILICATE	7.3	5.0	8.5	3.6	0.0	0.0	24.4	0.46
CA AL-SILICATE	0.2	0.3	0.0	0.0	0.0	0.0	0.5	0.01
FE AL-SILICATE	0.1	0.1	0.0	0.0	0.0	0.0	0.2	0.01
K AL-SILICATE	1.0	0.7	0.0	0.0	0.0	0.0	1.7	0.03
PYRITE	3.3	1.8	0.0	0.0	0.0	0.0	5.1	0.10
BARITE	0.1	0.2	0.0	0.0	0.0	0.0	0.3	0.01
CA SILICATE	0.1	0.0	0.0	0.0	0.0	0.0	0.1	0.00
CA ALUMINATE	0.1	0.1	0.3	0.0	0.0	0.0	0.6	0.01
RUTILE	0.2	0.6	0.0	0.0	0.0	0.0	0.8	0.02
DOLOMITE	0.0	0.0	0.7	0.0	0.0	0.0	0.8	0.02
PYRRHOTITE/SULFA	0.1	0.0	0.0	0.0	0.0	0.0	0.1	0.00
CA-RICH	0.1	0.0	0.0	0.0	0.0	0.0	0.1	0.00
SI-RICH	0.1	0.1	0.0	0.0	0.0	0.0	0.2	0.00
UNKNOWN	1.2	1.7	0.0	2.1	0.0	0.0	5.0	0.10
TOTAL	22.3	20.1	19.2	19.0	19.4	0.0	100.0	1.89

TABLE 6

SUMMARY OF CCSEM RESULTS FOR BEULAH FUEL

	Weight Percent Mineral Basis Particle-Size Distribution (μm)							Total wt.%
	<2.2	2.2-4.6	4.6-10	10-22	22-46	>46	Total	Coal Basis
QUARTZ	16.8	6.2	0.9	1.5	2.8	4.6	32.8	0.08
IRON OXIDE	1.3	2.7	0.0	0.0	0.0	0.0	4.1	0.01
ALUMINOSILICATE	1.8	1.6	0.0	2.2	0.0	0.0	5.6	0.01
CA AL-SILICATE	0.2	0.1	0.0	0.0	0.0	0.0	0.3	0.00
FE AL-SILICATE	0.1	0.1	0.0	0.0	0.0	0.0	0.2	0.00
K AL-SILICATE	0.2	1.0	0.0	0.8	0.0	0.0	2.0	0.01
PYRITE	10.3	3.1	2.8	0.0	0.0	0.0	16.1	0.04
GYPSUM	0.2	0.5	0.4	0.3	0.0	0.0	1.3	0.00
CA SILICATE	0.1	0.6	0.0	0.0	0.0	0.0	0.7	0.00
GYP/AL SILICATE	0.0	0.0	0.0	1.6	2.1	0.0	3.8	0.01
CA ALUMINATE	0.1	0.0	0.0	0.0	0.0	0.0	0.1	0.00
RUTILE	0.2	0.4	0.0	0.0	0.0	0.0	0.6	0.00
PYRRHOTITE/SULFA	0.1	0.0	0.0	0.0	0.0	0.0	0.1	0.00
CA-RICH	0.0	0.1	0.0	0.0	0.0	0.0	0.1	0.00
SI-RICH	0.3	0.1	0.0	0.3	0.0	0.0	0.7	0.00
UNKNOWN	2.4	1.4	0.9	6.5	20.3	0.0	31.5	0.08
TOTAL	34.1	17.9	5.0	13.2	25.3	4.6	100.0	0.24

CCSEM analysis, most of the 2.56% ash in the Beulah was either organically bound or less than 1 μm in average diameter, the lower detection limit of CCSEM. The Beulah organically bound fraction has much larger quantities of Fe_2O_3 and CaO than the other coals, and only a fraction of these components are accounted for by discrete minerals. The Fe_2O_3 and CaO may act as fluxing agents, effectively lowering the ash fusion temperature in an aluminosilicate system. This would help induce slag and deposit formation at the 2000°F temperatures present in the gas turbine simulator. Ash fusion temperatures were much lower for the Beulah-Zap as compared to the other test coals. Chemical fractionation analysis may need to be done on the Beulah coal to determine the portion of inorganic constituents that remain organically bound.

The importance of the CCSEM results as an interpretative tool is more evident when combined with the ash content and composition of the fuels. It can be argued that a larger particle-size distribution of minerals in coal can significantly increase subsequent fly ash particle impaction rates on turbine blades, which in turn increases the potential for deposit development. Larger quantities of minerals were noted in the >10 μm range for the Beulah (43%) and the Kemmerer (38%) fuel, as compared to the Otisca (0%) fuel on a mineral basis, which is consistent with the deposition seen in the turbine simulator.

5.0 FUTURE PLANS

Future plans include finishing the construction of the HTHP cyclone vessel, conducting a hydrostatic pressure test of the vessel, and casting the cyclone in refractory. The HTHP cyclone will be installed in the 1-MM Btu/hr gas turbine combustor and shakedown testing initiated. Spray tests in the pressurized spray chamber using previously tested CWF will be performed. Shakedown testing of the PDTF using the fuels previously tested in the gas turbine simulator will be accomplished. Future plans also include tests to look at what effects various levels of coal cleaning and different types of additives for increasing the ash melting temperatures have on the measured deposition rates and composition. A slurry feed system for the PDTF will be constructed, so fuel agglomeration tests can be completed.

6.0 REFERENCES

1. Swanson, M.L.; Mann, M.D.; Potas, T.A. "Comparison of Coal/Water Fuels Performance in a Gas Turbine Combustor"; Fourteenth International Conference on Coal & Slurry Technology; April 24-27, 1989, pp 353-364.

2. Swanson, M.L.; Moe, T.A.; Mann, M.D. "Advanced Coal Combustion"; Proceedings of the Sixth Annual Coal-Fueled Heat Engines and Gas Stream Cleanup Systems Contractors Review Meeting; March, 1989, pp 419-429, DOE/METC-89/6101.

3. Swanson, M.L.; Mann, M.D.; Moe, T.A. "Turbine Combustion Phenomena Annual Report"; April 1988 to July 1989, in press.

4. Benson, S.A.; Zygarlicke, C.J.; Toman, D.L.; and Jones, M.L. "Inorganic Transformations and Ash Deposition During Pulverized Coal Combustion of Two Western Coals"; ASME Ash Deposit and Corrosion Research Committee Seminar on Fireside Fouling Problems; Brigham Young University, Provo, Utah, April 4-6, 1990.

5. Perry, R.H.; Chilton, C.H. Chemical Engineer's Handbook; Fifth Edition, 1973, pp 20-81, 20-85.

6. Stairmand, C.J. Trans. Inst. Chem. Eng. **1951**, 29, 356.

7. Lapple, C.E. Ind. Hyg. Q. **1950**, 11, 40.